

PolyBlocks: A Compiler Infrastructure for AI Chips and Programming Frameworks

UDAY BONDHUGULA, Polymage Labs and Indian Institute of Science, India

AKSHAY BAVISKAR, Polymage Labs, India

NAVDEEP KATEL, Polymage Labs, India

VIMAL PATEL, Polymage Labs, India

ANOOP JS, Polymage Labs, India

ARNAB DUTTA, Polymage Labs, India

We present the design and implementation of PolyBlocks, a modular and reusable MLIR-based compiler infrastructure for AI programming frameworks and AI chips. PolyBlocks is based on pass pipelines that compose transformations on loop nests and SSA, primarily relying on lightweight affine access analysis; the transformations are stitched together in specialized ways to realize high-performance code automatically by the use of analytical cost models and heuristics. The optimizations in these passes include multi-level tiling, fusion, on-chip scratchpad usage, mapping matmuls and convolutions to matrix units, fusing the attention layer, and several other transformations for parallelism and locality. They have been developed in a way that makes it easy to build PolyBlocks-based compilers to target new chips, reusing much of the infrastructure. PolyBlocks' design and architecture enables fully automatic code generation from high-level frameworks to low-level target-specific intrinsics.

Experimental results from evaluating PolyBlocks-powered just-in-time compilation for PyTorch and JAX targeting NVIDIA GPUs show that it is able to match or outperform Torch Inductor and XLA in several cases, although the latter rely on a combination of vendor libraries and code generation. For individual operators like matmuls and convolutions, PolyBlocks-generated code is competitive with the best vendor-tuned libraries or hand-written kernels.

CCS Concepts: • **Software and its engineering** → **Just-in-time compilers; Retargetable compilers.**

Additional Key Words and Phrases: compilers, AI, MLIR

1 Introduction

Compilers are software systems that translate high-level program statements into instructions that the hardware can execute. With programming frameworks developing with higher-level abstractions and hardware chips with specialized features, compilers bridge larger gaps. For the domain of artificial intelligence (AI), there has been a rapid innovation in building specialized accelerator chips, with the desire to have high-level programming frameworks such as PyTorch [41, 52] and JAX [23] supported on them, while exploiting as much performance from the hardware as possible.

Tensorflow [1], PyTorch [41, 52], and JAX [23] are among the three dominant high-level frameworks to express ML and AI models. The standard way to execute these models is called *eager* execution. This involves executing the graph of tensor operators one after another, which the *executor* of the respective framework does by calling a pre-compiled and pre-optimized library routine available for the operator. A majority of high performance realized today from the execution of AI models comes from highly-optimized vendor libraries that the eager executors rely on. These include libraries such as MKL, OpenBLAS, CuDNN [11], CuBLAS, ROCm, FlashAttention [14], and TensorRT-LLM [26]. When developers are not satisfied with the performance delivered by

Authors' Contact Information: Uday Bondhugula, uday@polymagelabs.com, Polymage Labs and Indian Institute of Science, Bengaluru, Karnataka, India; Akshay Baviskar, Polymage Labs, Bengaluru, India; Navdeep Katel, Polymage Labs, Bengaluru, India; Vimal Patel, Polymage Labs, Bengaluru, India; Anoop JS, Polymage Labs, Bengaluru, India; Arnab Dutta, Polymage Labs, Bengaluru, India.

these libraries on GPUs, re-implementing the desired operators or a group of them with low-level abstractions like CUDA, Cutlass [53], Triton [55], C/C++ or inline assembly is common, requiring deeper optimization expertise and knowledge of the hardware.

Eager vs compiled: Besides the *eager* mode of execution described above, high-level frameworks like PyTorch, JAX, and Tensorflow also provide the *compiled* mode through other backends, often called the JIT (just-in-time) compiled mode. In the compiled mode, the graph of operators is captured, optimized, and processed as a whole, and code is generated for its various parts to a large extent. *Fusion* of operators is one of the greatest strengths of the compiled approach, reducing the number of trips made to the global memory, and in some cases even eliminating accesses to on-chip memory altogether. This greatly speeds up memory-bandwidth-bound computation, which is beneficial for nearly any chip. In addition, it also speeds up compositions of compute-bound operations (like matmuls, convolutions) with dependent memory bandwidth operations. Modern AI accelerators often include specialized hardware in the form of matrix units or tensor cores to dramatically speed up matrix-matrix multiplications. With Amdahl’s law, the balance tilts making optimization of other memory-bandwidth-bound computation important.

The PyTorch, JAX, and Tensorflow frameworks are served by different compilers that are effective separately for each. While TensorFlow and JAX have had XLA [24], Torch Inductor [2] has been reported to be the most effective for PyTorch [2] in terms of coverage and performance. These compilers do not share infrastructure beyond the lowest layers when targeting CPUs or GPUs. Supporting targets very different to CPUs or GPUs involves significant additional effort due to these compilers’ use of multiple different intermediate representations (IR) and their reliance on vendor libraries to realize performance for key operators, especially on CPUs and GPUs.

Programming landscape: high vs mid vs low-level frameworks: Although not standard terminology, we frequently use the *high*, *mid*, and *low* taxonomy in this paper to better describe the programming landscape for AI chips today. Popular programming approaches to develop and execute deep learning models fall into the following three categories: (1) low-level ones that include CUDA, OpenCL, C/C++ with abstractions such as Cutlass [53], (2) mid-level ones based on tile-level abstractions such as Triton [40, 55] and Pallas/Mosaic [25], and (3) high-level ones like PyTorch, JAX, and Tensorflow. Figure 1 illustrates how productivity and abstraction change across these. Compilers are employed for all three classes of frameworks, but the challenges of building them are vastly different. Compilation for PyTorch or JAX is more challenging than for a framework like Triton, with the former requiring more work in lowering abstractions.

Reliance on manually developed libraries vs fully code-generating: While Inductor, XLA, and TensorRT [26] are considered compilers, they rely on libraries for the most compute-intensive operators, sometimes heavily, when targeting CPUs and GPUs. For GPUs, they rely on CuDNN [11], CuBLAS, FlashAttention [14], and several other manually developed kernels. The opposite of this approach is a *fully code-generating* one, where the compiler generates all low-level code that is ultimately executed, where this low-level code is typically in the form of instructions and intrinsics for the hardware available in LLVM [43] or another low-level IR. The choice to use existing libraries may often be dictated by pragmatics since there has been no or little evidence of a high-level compiler generating code competitive with CuDNN (for convolutions), or CuBLAS (for matmuls), or kernels for the attention [58] layer. The automatic transformation and optimization ability needed to realize that level of performance in a reusable way involves substantial effort. In addition, significant effort may have already been put into building such libraries, and layering on top of such libraries provides a separation of concerns. However, there are also major downsides to using libraries in the long term: (1) they become non-portable due to various versions and strategies needed for different problem sizes and targets, choices that could have been encoded into a fully

low-level and mid-level optimization approaches and even vendor-tuned libraries on NVIDIA GPUs. More importantly, the PolyBlocks infrastructure allows one to quickly build compilers for new AI chips without the need to redevelop several advanced transformations. When used as a backend for PyTorch, JAX, or TensorFlow for GPUs, it provides significant improvements in several cases over state-of-the-art approaches that rely on both libraries and code generation.

The remainder of this paper is organized as follows. In Section 2, we describe the various design choices we made for PolyBlocks. Section 3 describes the high-level architecture of PolyBlocks. Section 4 describes in detail some of the key optimizations available in PolyBlocks. Experimental evaluation and performance comparison are provided in Section 5. Related work and conclusions are presented in Section 6 and Section 7 respectively.

2 Design Choices

Building a compiler infrastructure that spans the distance between high-level frameworks and specialized chips presents multiple choices in various steps. In this section, we discuss the design choices we made and their rationale. Our objective here is to build an infrastructure for high-level frameworks that provides an abstraction similar to that of TensorFlow, PyTorch, and JAX.

The presence of multiple levels of parallelism, matrix units or tensor cores, vector units, and on-chip memory or scratchpads of various kinds that require explicit data movement are common features of various specialized accelerators. The ability to overlap computation and data movement is also important. The gap between global memory bandwidth and compute speed also necessitates cross-operator fusion to maximize reuse in on-chip memory and registers.

Full automation first: There have been various approaches to compiling deep learning computations, with different IRs, with programmer-supplied schedules, and reliance on auto-tuning. With schedule-driven approaches, the optimization of models was guided by a schedule of transformations separate from the specification. The schedule would be different for not only different hardware but also different inputs. This process requires experts who are knowledgeable about both compute patterns and the target hardware throughout the optimization process. In some way, humans become part of the compiler. We deliberately avoided this approach, as it is not sustainable or scalable when dealing with the cross-product of evolving models and hardware. Our focus is on full automation to start with. However, this choice does not preclude us from tuning or controlling various parameters in the cost model for future purposes if input is desired. We also wished to avoid relying on auto-tuning early on during the development to restrict tuning to a very focused space and to reach that space through the maturity of the compiler infrastructure and the cost models used.

Fully code-generating approach: For the reasons related to fusion, maintainability, scalability, and extensibility to new hardware that were discussed in Section 1, we consciously avoided relying on hand-written libraries, closed or open source, by choosing to build a fully code-generating compiler all the way to target-specific intrinsics available. This allows the developed passes and transformations to be more reusable each time new hardware is to be supported, since newer hardware may not have libraries as well-developed or mature as for the NVIDIA GPU ecosystem today.

Reusable pass pipeline-based approach: All of the above leads us to an approach where we built a number of transformation passes for various key pieces. Before the availability of the MLIR [29, 35] intermediate representation (IR) infrastructure in 2019, we believe that the basic toolkit to build compilers to traverse the entire abstraction distance from high-level representations to generate code for hardware target intrinsics was not available. In order to maximize reusable infrastructure, we structured it as a sequence of MLIR pass pipelines, through which all IR, regardless

of the input framework, go. Nearly the same pipelines are used across different hardware up to the mid-level stages. More detail on this is provided in the next section.

Incremental programmability: one-line compile directive: Our desire was to make compilation equivalent to turning a switch on or off. Usability would thus be similar to that of models like OpenMP. Both Torch Inductor [2] and XLA JIT [24] provide such a user experience, which is highly productive, with the eager mode co-existing for initial debugging, reference, and validation purposes. As shown in Figure 2, compilation is enabled by a one-line directive on the desired function, either through an annotation or an API call. With this approach, unmodified PyTorch, JAX, or Tensorflow models can be compiled and executed.

```
@polyblocks_jit_torch(compile_options={'target': 'nvgpu'})
def blur_x_blur_y(img):
    # We are doing a regular image convolution in the
    # X direction and then in the Y direction.
    blur_kernel = kernel.view(1, 1, 1, 5)
    img_resaped = img.view(3, 1, height, width)
    # The output is two short at each end.
    blurx = torch.nn.functional.conv2d(img_resaped,
                                       blur_kernel, stride=1, padding=0)
    blur_kernel = kernel.view(1, 1, 5, 1)
    blury = torch.nn.functional.conv2d(blurx, blur_kernel,
                                       stride=1, padding=0)
    output = blury.view(3, height - 4, width - 4)
    return output

out = blur_x_blur_y(img)

def attention(self, q, k, v, bias):
    k_t = torch.transpose(k, -1, -2)
    qk = torch.matmul(q, k_t)
    qk = qk + bias
    soft_qk = torch.nn.functional.softmax(qk,
                                          dim = -1)
    res = torch.matmul(soft_qk, v)
    return res

compiled = torch.compile(attention,
                          backend="polyblocks",
                          options={"target": "nvgpu"})
```

(a) 3x of Torch Inductor on NVIDIA A10.

(b) PolyBlocks is registered as a Torch backend.

Fig. 2. PyTorch functions JIT compiled with PolyBlocks. Incremental programmability.

Reliance on built-in MLIR dialects and type system: We found the MLIR type system sufficient for all the core transformations, including target-specific mid-level transformations. We consciously avoided adding new dialects or operations for such purposes. These choices allowed optimizations and lowerings to be available to a large class of higher-level operations that were lowered to affine nests, and a resilience to input lowered from different programming frameworks. We make use of external attributes over short distances in the pass pipeline to convey information and hints to heuristics and to avoid recomputation of certain properties (Appendix A.4).

Use of affine or polyhedral techniques only where needed: Polyhedral techniques [5, 8, 59, 60] are powerful in resolving a large number of analyses arising from mid-level transformations such as fusion, tiling, and generation of data movement code between fast and slow memories. However, they also rely on relatively expensive integer set operations, which are often an overkill for many analyses when dealing with IR lowered from tensor operators. A large number of cases are resolved with simple linear or constant time checks on affine functions, and one has to defer to more expensive polyhedral operations in a small set of cases. We also note that several of the models that we compile and report performance for, or desire to scale to have up to tens of thousands of loop nests (hundreds or a few thousands of named tensor operators at the level of torch aten, mhlo, or stablehlo dialects). To make compiler development practical, we believe that compile times have to be kept to the order of a few seconds to a few tens of seconds, even for the largest models we see today.

3 Architecture

In this section, we describe the architecture of the PolyBlocks core engine and the template architecture of any compiler built with PolyBlocks. The reader is referred to the literature on

MLIR [35], [29] since the rest of this section, in various places, assumes familiarity with the MLIR concepts of dialects, operations, built-in types, and its use of SSA.

3.1 Choice of dialects and lowering paths

Figure 3 shows the lowering paths through dialects. It is not meant to be fully exhaustive, but close to capturing lowering paths through edges. All three frameworks, TensorFlow, PyTorch, and JAX, have had entry paths into MLIR [29, 35] for several years maintained by open-source community-driven projects. The Tensorflow project includes a customizable pass pipeline that lowers from the *tf* dialect to the *mhlo* dialect after *tf.functions* are imported into the *tf* dialect. For JAX, the JAX JIT API provides a way to lower JAX graphs to the *stablehlo* dialect. For PyTorch, Torch dynamo is used to capture FX graphs, which can then be lowered by the *torch-mlir* [30] project: from the *torch* dialect through *aten* to *linalg*. The *mhlo*, *stablehlo*, and *linalg* dialects thus form the entry point into the PolyBlocks compiler engine. Any combination of these dialects can be handled seamlessly. All of these dialects operator on MLIR *tensor* types and thus tensor value semantics are used. Tensors are SSA values and can only be defined once. On these lowering paths until the mix of *mhlo*, *linalg*, and *stablehlo*, the PolyBlocks compiler driver uses additional customization whenever an alternate lowering is desirable. In such cases, the *polyblocks* dialect is used to add a path for such operations.

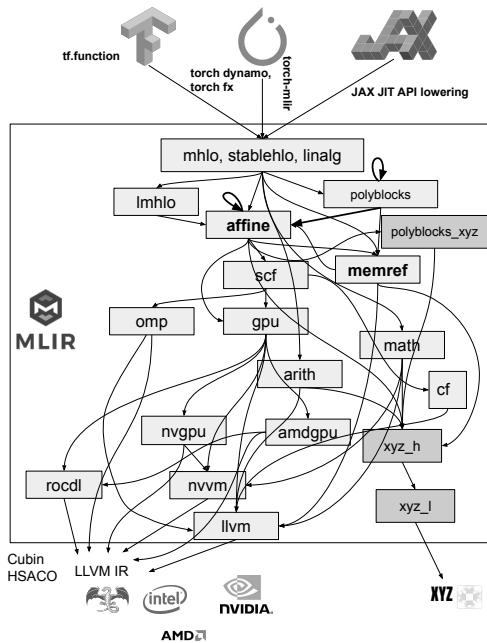


Fig. 3. PolyBlocks compiler engine powering multiple programming frameworks and hardware. MLIR dialect lowering paths and how new targets are supported (XYZ in this figure).

3.2 A five-stage pass pipeline

The PolyBlocks lowering and transformation infrastructure is organized as a five-stage pass pipeline shown in Figure 4: S1 through S5 for proper isolation, organization, and easier debugging purposes.

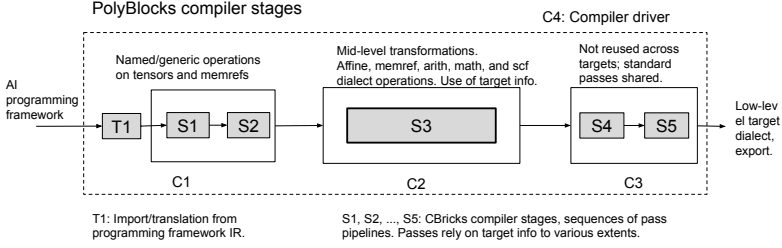


Fig. 4. Overall components and high-level architecture of a compiler built from PolyBlocks.

Frontend stage: The S1 and S2 stages are nearly target neutral. The S1 stage lowers from operations on *tensor* types to those on *memref* types, i.e., buffer semantics are introduced. The S2 stage lowers from named ops on *memref* types to affine loop nests. Very little target-specific information is used by S1 and S2, and is often restricted to supplying information on precision modes (e.g., using mixed-precision) or providing supported matmul precision modes to specific passes, which may need this information where lowering or expanding named ops.

Mid-level optimizer: The S3 stage is the mid-level optimizer where the majority optimizations and mappings are performed, relying on target information to various extents. The S3 pass pipeline comprises 50-70 passes typically for a target. It operates primarily on the *affine* [45] and *memref* dialect with the ability to realize specialized code for a target, while still using MLIR’s in-built type system. Fusion, tiling, mapping to matrix units, generation of data movement code for on-chip memories, and vectorization are performed in S3. Standard dialects from MLIR like *arith*, *math*, *builtin*, and *func* are used throughout in most stages. Operations from the *vector* dialect are used as a result of the vectorization.

Backend stages: The S4 stage converts from the *affine* and *memref* form to the *scf* dialect in conjunction with other target-specific dialects where special abstractions are needed to represent parallelism and synchronization. For GPUs, this is the *gpu* dialect, and the *omp* dialect for CPU parallelization. The S5 stage then lowers the *scf* and other target-specific parallelism abstractions out of MLIR. For NVIDIA GPUs, this would lower to LLVM + NVVM through the *nvgpu* dialect (or through the *amdgpu* dialect for AMD GPUs), and to LLVM for CPUs. Component C3, which includes S4 and S5 is very target-specific and these are not reused across targets beyond standard upstream passes like canonicalization, dead code elimination, CSE, and invariant code motion.

Compiler driver: Finally, all three components, C1, C2, and C3, are combined by a compiler driver (C4), which is developed in Python. C4 defines the pass pipeline specifications for all the different stages, passing IR through these different stages, providing target information, and providing other debugging capabilities. C4 includes the support to convert the graph representations of the programming frameworks’ to MLIR, leveraging existing open-source infrastructure (T1). C4 crucially also contains the logic to process input and output data when performing JIT compilation, i.e., converting between the programming frameworks’ tensor representation to the memref ABI that the compiled MLIR uses. Support for ahead-of-time compilation is also handled here, where a binary or a library can be generated for the specification being supplied. MLIR’s LLVM ORC-based [44] execution engine is used to execute the compiled code to realize the JIT for both CPUs and GPUs while linking the desired runtime libraries. For other targets, available custom runtime paths and their Python bindings are used to create the execution driver in C4. For NVIDIA GPUs, MLIR’s LLVM with NVVM intrinsics are translated through LLVM’s optimization pipeline through to its NVPTX backend and subsequently to GPU assembly through the CUDA driver API. The CUDA runtime is the only dependency for the executable code for NVGPUs and the ROCm runtime

similarly for AMD GPUs. For CPUs, the OpenMP runtime is dynamically linked, while LLVM’s OpenMP support is leveraged for the generated code.

Building a new PolyBlocks-based compiler: Due to the above organization, we have the following powerful properties and well-isolated separation when creating new target backends for PolyBlocks. Building a new compiler with PolyBlocks requires: (1) almost reusing everything as is from T1, S1, and S2, (2) customizing the passes of S3 for the new target, (3) building out S4 and S5 from scratch (reusing standard canonicalization, low-level optimization passes), and (4) support in C4 for input/output, kernel launching, and synchronization.

4 Optimizations

In this section, we describe some of the key components of the mid-level optimizer, and how we built or derived passes based on upstream MLIR infrastructure. As mentioned in the previous section, the dialects in bold in Figure 3 is where most of the transformation and optimization described in the next section is performed. The use of *affine* and *memref* dialects allows us to perform transformations in a very generic and powerful way, resilient to changing patterns in the input programming frameworks. Different kinds of convolutions, matmuls, and tensor contractions, which might have been lowered from different kinds of ops and differently named ops in programming frameworks, are all optimized to the same extent, as our results and performance improvements will later demonstrate. All code snippets shown in this section are from PolyBlocks-generated IR.

4.1 Use of affine analysis for various purposes

For various transformations, PolyBlocks relies on analysis of affine memory access patterns. In this section, we show a simple example.

Consider the access to the 4-d tensor load in Figure 5. Does the access have contiguity along loop IV ‘%j’? Affine expressions, maps, and load/store operations in MLIR’s affine dialect make such analysis easy. The transcript has four dimensions, and ‘%j’ appears in both the third and fourth dimensions. Most low-level compilers’ analyses are unable to reason about vectorizability here. Although the penultimate subscript also changes with ‘%j’, the access does exhibit spatial reuse in intervals of two, but not in intervals of four or eight. As a result, it can be vectorized to use 2xf16 vector loads, which PolyBlocks’ vectorization pass performs given target information. This is an example of simple near O(n) time checks (in the IR expression lengths) that can resolve contiguity analysis queries.

```

affine.for %i = 0 to 32 {
  affine.for %j = 0 to 32 {
    %v = affine.load memref[(%i + %ii * 32) floordiv 519684,
      ((%i + %ii * 32) mod 519684) floordiv 254) * 2 + (((%j + %jj * 32) floordiv 10) mod 16) floordiv 4,
      (%i + %ii * 32) mod 254) * 2 + ((%j + %jj * 32) floordiv 10) mod 4,
      (%j + %jj * 32) mod 10
    ] : memref<8x4094x510x10xf16>
    affine.store %v, %13[%i, %j] : memref<32x40xf16, 3>
  }
}

```

Fig. 5. A specialized packing into an on-chip memory buffer: note contiguity in two-sized intervals along %j.

4.2 Slicing-based affine fusion

The goal of this section is to first provide a high-level background of slicing-based affine fusion, the basic infrastructure of which has been available in the official MLIR repository. We do not claim that as a contribution of this work. We describe how that infrastructure was customized and extended to build a fusion pass in PolyBlocks with various heuristics and cost modeling with extensibility for other targets.

Slicing-based fusion goes beyond traditional loop fusion [28, 62] in the compiler literature. For a given producer-store (the source), a consumer load (the destination) and a given destination loop depth to fuse into, the approach computes the slice of the producer that is to be executed to provide the dependent data to the consumer. Consequently, the producer can be pulled in and materialized to compute the required memref locations at that depth, leading to a shorter reuse distance, a smaller temporary, or elimination of the temporary (register reuse in the case of innermost fusion). Conversely, a consumer can be pulled into the producer with a similar approach. Our fusion pass supports both the producer-into-consumer and the consumer-into-producer fusion. Unlike traditional loop fusion, slicing-based fusion can lead to the introduction of redundant computation, which has to be carefully controlled through a cost model, for e.g., 0-10% of redundant computation can be tolerated.

To determine the validity of such slicing-based fusion precisely, various checks need to be performed, including the presence of intervening conflicting memory operations and whether the source can be safely erased post-fusion. In a very small set of cases, we end up using the integer set library [59, 61] when simpler techniques are insufficient. This usage can be replaced with the FPL library [21, 42] already available in MLIR when the latter has support on par with ISL. To compute the slice itself, affine memory dependence constraints are used to express the slice in terms of the destination loop iterators.

While evaluating a specific fusion, we consider criteria such as preservation of parallelism, preservation of vectorizability, the amount of redundant computation added, and whether the fusion will eventually lead to the elimination of intermediate buffers, i.e., the creation of a private memref or a scalar in the case of register-level (typically innermost loop) fusion, and whether the size of private memref fits in available fast chip memory. We also make use of CBrick kinds (Section A.4) to speed up the checks and eliminate undesirable fusion with a simple set of rules. For example, the fusion between two matmul or two reduction cbrick kinds is not attempted, except separately in scenarios covered in Section 4.4. Similarly, the fusion of any non-trivial operation into broadcasting consumers is disallowed.

In Figure 6, a fusion is performed between two stencil-like operations that leads to an imperfect nest and the creation of a 3 KB buffer (%alloc_7) in the local on-chip memory, completely eliminating a trip to global memory and a global memory allocation. Both XLA and Inductor are unable to perform such fusion across such operators. This specific fusion is easily performed as a result of modeling on affine nests (potentially imperfectly nested) and affine memory operations. The stencils here were lowered forms from depth-wise convolution operators expressed in PyTorch. For GPUs, IR such as this leads to a single fused kernel.

4.3 Multi-level tiling and fusion approach

While it is well-known how to perform tiling on loop nests, its interplay with fusion is complex. The end-result one desires is a nest that is tiled and fused. However, neither fusing and then tiling, nor tiling and then fusing, is sufficient in general and in many important cases; both could lead to undesirable results. Consider the situation of slicing-based fusion. The slice that is being pulled in gets effectively tiled as per its destination. The tiling expressed on the source nest, if any, would be lost. It is thus sufficient to tile the destination appropriately and then pull in untiled sources (producers or consumers).

Two-phase approach: Tiling a nest that will be the destination of subsequent fusions, either of its producers or of its consumers, is thus the first key step. Once all fusions determined to be profitable into such tiled nests are performed, the remaining nests can be tiled either for locality or parallelism purposes. We follow such a two-round approach. We first tile a set of key nests, which typically include all matmuls, convolutions, and destination stencils. We then perform the

```

affine.for %i = 0 to 3 {
  affine.for %j = 0 to 4096 {
    affine.for %k = 0 to 4092 {
      affine.store %cst_3, %0[%i, %j, %k] : memref<3x4096x4092xf32>
    }
  }
} {polyblocks.kind = "broadcast", polyblocks.target = "gpu"}
affine.for %i = 0 to 3 {
  affine.for %k = 0 to 4096 {
    %7 = affine.load %arg0[%i, %j, %k] : memref<3x4096x4096xf32>
    %8 = affine.load %0[%i, %j, %k] : memref<3x4096x4092xf32>
    %9 = arith.mulf %7, %cst_1 : f32
    %10 = arith.addf %8, %9 : f32
    %11 = affine.load %arg0[%i, %j, %k + 1] : memref<3x4096x4096xf32>
    %12 = arith.mulf %11, %cst_0 : f32
    %13 = arith.addf %10, %12 : f32
    %14 = affine.load %arg0[%i, %j, %k + 2] : memref<3x4096x4096xf32>
    %15 = arith.mulf %14, %cst : f32
    %16 = arith.addf %13, %15 : f32
    affine.store %16, %0[%i, %j, %k] : memref<3x4096x4092xf32>
  }
}
} {polyblocks.kind = "stencil", polyblocks.target = "gpu"}
%1 = memref.alloc() : memref<3x4092x4092xf32>
affine.for %i = 0 to 3 {
  affine.for %j = 0 to 4092 {
    affine.for %k = 0 to 4092 {
      affine.store %cst_3, %1[%i, %j, %k] : memref<3x4092x4092xf32>
    }
  }
}
} {polyblocks.kind = "broadcast", polyblocks.target = "gpu"}
affine.for %i = 0 to 3 {
  affine.for %j = 0 to 33 {
    affine.for %k = 0 to 682 {
      affine.for %l = 0 to 1 {
        affine.for %m = 0 to 124 {
          affine.for %n = 0 to 6 {
            %7 = affine.load %0[%i + %l, %m + %j * 124,
              %n + %k * 6] : memref<3x4096x4092xf32>
            %8 = affine.load %1[%i + %l, %m + %j * 124,
              %n + %k * 6] : memref<3x4092x4092xf32>
            %9 = arith.mulf %7, %cst_1 : f32
            %10 = arith.addf %8, %9 : f32
            %11 = affine.load %0[%i + %l, %m + %j * 124 + 1,
              %n + %k * 6] : memref<3x4096x4092xf32>
            %12 = arith.mulf %11, %cst_0 : f32
            %13 = arith.addf %10, %12 : f32
            %14 = affine.load %0[%i + %l, %m + %j * 124 + 2,
              %n + %k * 6] : memref<3x4096x4092xf32>
            %15 = arith.mulf %14, %cst : f32
            %16 = arith.addf %13, %15 : f32
            affine.store %16, %1[%i + %l, %m + %j * 124,
              %n + %k * 6] : memref<3x4092x4092xf32>
          }
        }
      }
    }
  }
}
} {polyblocks.kind = "stencil", polyblocks.target = "gpu"}

```

```

affine.for %i = 0 to 3 {
  affine.for %j = 0 to 33 {
    %alloc_7 = memref.alloc() : memref<1x126x6xf32, 3>
    affine.for %l = affine_map<(d0) -> (d0 * 124)>(%j)
      to affine_map<(d0) -> (d0 * 124 + 126)>(%j) {
        affine.for %m = affine_map<(d0) -> (d0 * 6)>(%k)
          to affine_map<(d0) -> (d0 * 6 + 6)>(%k) {
            affine.store %cst_3, %alloc_7[0, %j * -124 + %l,
              %k * -6 + %m] : memref<1x126x6xf32, 3>
            %0 = affine.load %arg0[%i, %l, %m]
              : memref<3x4096x4096xf32>
            %1 = arith.mulf %0, %cst_1 : f32
            %2 = arith.addf %1, %cst_3 : f32
            %3 = affine.load %arg0[%i, %l, %m + 1]
              : memref<3x4096x4096xf32>
            %4 = arith.mulf %3, %cst_0 : f32
            %5 = arith.addf %2, %4 : f32
            %6 = affine.load %arg0[%i, %l, %m + 2]
              : memref<3x4096x4096xf32>
            %7 = arith.mulf %6, %cst : f32
            %8 = arith.addf %5, %7 : f32
            affine.store %8, %alloc_7[0, %j * -124 + %l,
              %k * -6 + %m] : memref<1x126x6xf32, 3>
          }
        }
      }
    }
  }
}
affine.for %l = 0 to 1 {
  affine.for %m = 0 to 124 {
    affine.for %n = 0 to 6 {
      affine.store %cst_3, %alloc[%i + %l, %j * 124 + %m,
        %k * 6 + %n] : memref<3x4092x4092xf32>
      %0 = affine.load %alloc_7[%l, %m, %n]
        : memref<1x126x6xf32, 3>
      %1 = arith.mulf %0, %cst_1 : f32
      %2 = arith.addf %1, %cst_3 : f32
      %3 = affine.load %alloc_7[%l, %m + 1, %n]
        : memref<1x126x6xf32, 3>
      %4 = arith.mulf %3, %cst_0 : f32
      %5 = arith.addf %2, %4 : f32
      %6 = affine.load %alloc_7[%l, %m + 2, %n]
        : memref<1x126x6xf32, 3>
      %7 = arith.mulf %6, %cst : f32
      %8 = arith.addf %5, %7 : f32
      affine.store %8, %alloc[%i + %l, %m + %j * 124,
        %n + %k * 6] : memref<3x4092x4092xf32>
    }
  }
}
} memref.dealloc %alloc_7 : memref<1x126x6xf32, 3>
}
} {polyblocks.kind = "stencil", polyblocks.target = "gpu"}

```

(a) Original code.

(b) Fused code.

Fig. 6. Affine slicing-based fusion. The first stencil nest is pulled into the second one by computing the producer slice needed by the consumer. Fusion happens into right under the 682-iteration %k loop of Figure 6(a), i.e., given an %i, %j, %k, the slice of the producer needed.

slicing-based fusion described in Section 4.2 on all nests. In the second round, all remaining untiled nests are tiled. With this approach, the fusion of pointwise nests with other pointwise nests happens in their untiled form, which is simple and straightforward. Fusion into matmuls and convolutions happens into tiled nests.

Fusion into matmuls and convolutions has to happen after the generation of fast buffers, i.e., global to on-chip memory movement code generation. As such, fast buffer generation for matmuls and convolutions is performed early. Fusion subsequently happens into the copy-in and copy-out nests of such tiled nests, which is the desired outcome. Data movement code generation for the remaining nests where accesses exhibit temporal reuse is performed late in the pipeline.

Each level of parallelism represented by a contiguous band of *affine.for* loops is turned into a multi-dimensional *affine.parallel* operation after all desired optimization on ‘affine.for’ nests (cf. Figure 8). The interactions between tiling and fusion also require careful consideration in the selection of tile sizes and the choice to generate fast buffers (whether to use on-chip memory for a specific memref/access) since the eventual on-chip memory utilization changes after fusion has been performed. Our pipeline is able to spill buffers from fast memory to global memory much later in its stages if the utilization goes beyond the on-chip memory capacity, something that may rarely happen due to the inability to model interactions between passes that are distant in the pipeline.

4.4 Fusion and tiling of the attention layer

In this section, we describe how we automatically achieve the fusion of all operations in the attention layer [58] through a composition of simpler loop and code motion transformations. The fusion required here to achieve state-of-the-art performance [13] is normally outside the scope of both standard compiler fusion [28, 62], slicing-based fusion techniques [24, 49, 64], including those described in Section 4.2 or any other techniques that rely on data dependences. Note that such a fusion can be realized only because it is possible to compute the softmax part online [34]. PolyBlocks primarily employs two optimization passes for this purpose, *reduce-reduce-fusion* and *wnma-fusion*, to minimize expensive memory accesses in an attention layer computation. These passes target DRAM and on-chip memory accesses, respectively, specifically addressing the large output of $Q * K^T$.

The reduce-reduce-fusion pass operates on the attention layer, which is initially represented as a sequence of affine nests. The pass’s objective is to fuse these nests into a single affine nest. It identifies a series of nests for fusion based on heuristics that consider factors such as matrix multiplication problem sizes, the number of intervening reduction nests and their interdependencies. Memory dependences among identified nests form a directed acyclic graph (DAG). The reduce-reduce-fusion pass fuses them into the sink node in reverse topological order. A notable challenge is in supporting the fusion of a producer reduction nest into a consumer reduction nest within a consumer reducing loop. This is crucial to achieve good performance for the attention layer. However, such a fusion violates memref dependences on the result memref of the producer reduction. To overcome this, the fusion is performed despite the dependence, and additional operations are then introduced to preserve the original program semantics. Our approach automatically extracts the necessary correction computation from the fused nest. This correction is then inserted right before the consumer reduction load, ensuring that the consumer reduction result remains consistent with the last executed iteration of the reduction loop.

In the output of the reduce-reduce-fusion pass, a consumer reduction result is corrected whenever a producer reduction result is updated. However, this correction should only occur once per tile of the producer reduction result to minimize computational overhead. To achieve this, we employ a second pass called *attention-matmul-outlining*. This pass transforms a tiled fused-attention nest, outlining the matrix multiplications and separating the correction computation from the reduction.

Our reduce-reduce-fusion pass can handle the Attention variations supported by FlexAttention [18] with little to no extra effort, because many of the variations supported by FlexAttention, when lowered to affine nests, result in one or more pointwise nests operating on the output of $Q * K^T$, and generating an input for the subsequent softmax part, and the fusion of which is already supported by our fusion utilities.

wmma-fusion: While the reduce-reduce-fusion pass eliminates DRAM round-trips for the output of the *Query* and *Value* matrix multiplication, achieving peak performance also necessitates avoiding round-trips to on-chip memory. This is where a third pass comes into play, the wmma-fusion pass. This pass works on a fused attention nest that comprises the two matrix multiplications, along with other nests required for softmax computation and the “correction” operations. At this stage, all nests are fetching data from on-chip memory, and the matrix multiplication nests have already been mapped to matrix units if any (Warp Matrix Multiply-Accumulate operations in the case of NVIDIA/AMD GPUs). The wmma-fusion pass first maps all non-matmul nests within the fused attention to WMMA/matrix operations, ensuring compatibility with the existing matmul mappings. This mapping is facilitated by our matrix-mapping utilities. Once all nests are mapped, they are fused into the first matrix multiplication using existing fusion utilities (Section 4.2). The fused nest is then fully unrolled, and scalar replacement is performed, effectively eliminating round-trips to on-chip shared memory, i.e., results are fully reused within registers.

4.5 Transforming and mapping convolutions with on-the-fly packing

It is well-known that convolutions can be computed using matrix multiplication operations. The left-hand side (LHS) and right-hand side (RHS) of the matrix multiplication are constructed using the input image and filter weights, respectively. Each row of the LHS matrix is formed by flattening the image elements overlapped by the kernel window, and each column of the RHS matrix is formed by flattening the elements in the kernel window. Explicit GEMM and implicit GEMM are two terms used to specify whether such a reorganization is performed globally on the data or on-the-fly on tiles.

Materializing the LHS matrix can cause significant memory overhead due to overlaps in the sliding window. Employing on-the-fly packing as shown in Figure 7b addresses this issue, where we form a tile of the LHS matrix in the fast memory by loading the required elements from the original image tensor. Similarly, a tile of the RHS matrix is formed using the filter weights. Later, matrix multiplication is performed on the LHS and RHS tiles, and the elements of the output matrix are stored back to the original output tensor. We perform such a transformation by first generating a 3-d loop form of the matrix multiplication nest (Figure 7a) that operates on the original tensors, but with the right affine accesses. Later, this nest is tiled and fast buffers are generated to realize on-the-fly packing shown in Figure 7b.

Partial tiles are formed if the dimension of the resultant matrices is not a multiple of the chosen tile size or the hardware-supported matrix unit. To ensure correct results, we pad the partial contracting dimension of the LHS tile with zeros in the fast memory (Figure 7b).

Note that no new operations were required in MLIR to realize this transformation. Also, this transformation works for all 2-d convolutions with different configurations (stride, dilation, and padding kinds) and transpose convolutions as well. The evaluation presented in Section 5 exercises all of this.

A related approach is the implicit GEMM algorithm included with Cutlass [3]. However, to the best of our knowledge, none of the existing high-level compilers are able to auto-generate such a packing and mapping from loop nests for the entire diversity of convolutions.

```

affine.for %i = 0 to 3528 step 128 {
  affine.for %j = 0 to 512 step 128 {
    %input_fast_buf = memref.alloc() : memref<128x32xf16, 3>
    %weights_fast_buf = memref.alloc() : memref<32x128xf16, 3>
    %output_fast_buf = memref.alloc() : memref<128x128xf32, 3>
    // Output packing nest.
    affine.for %ii = 0 to min affine_map<(d0) -> (128, -d0 + 3528)>(xi) {
      affine.for %jj = 0 to 128 {
        %0 = affine.load %output_memref[(xi + %ii) floordiv 441, ((xi + %ii) mod 441) floordiv 21,
          (xi + %ii) mod 21, %j + %jj] : memref<8x21x21x512xf32>
        affine.store %0, %output_fast_buf[%ii, %jj] : memref<128x128xf32, 3>
      } (polyblocks.parallel)
    } (copy_nest, polyblocks.parallel)
    affine.for %k = 0 to 1143 step 32 {
      // Input packing nest.
      affine.for %ii = 0 to 128 {
        affine.for %kk = 0 to 32 {
          %0 = affine.load %image_memref[(xi + %ii) floordiv 441] mod 8,
            (((xi + %ii) mod 441) floordiv 21) + 2 + ((k + %kk) floordiv 127) floordiv 3,
            ((xi + 2 + %ii) - ((xi + %ii) floordiv 21) + 42 + (k + %kk) floordiv 127
              - (((k + %kk) floordiv 127) floordiv 3) + 3) mod 44,
            ((k + %kk) mod 127) : memref<8x44x44x127xf16>
          affine.store %0, %input_fast_buf[%ii, %kk] : memref<128x32xf16, 3>
        } (polyblocks.parallel)
      } (copy_nest, polyblocks.parallel)
      // Weights packing nest.
      affine.for %kk = 0 to 32 {
        affine.for %jj = 0 to 128 {
          %0 = affine.load %weights_memref[(((k + %kk) floordiv 127) floordiv 3) mod 3,
            ((k + %kk) floordiv 127) mod 3,
            ((k + %kk) mod 127, %j + %jj] : memref<3x3x127x512xf16>
          affine.store %0, %weights_fast_buf[%kk, %jj] : memref<32x128xf16, 3>
        } (polyblocks.parallel)
      } (copy_nest, polyblocks.parallel)
      // Zero pad the partial tile in the fast memory.
      affine.for %kk = 1143 to affine_map<(d0) -> (d0 + 32)>(kk) {
        affine.for %jj = 0 to 128 {
          affine.store %zero, %weights_fast_buf[%kk - %k, %jj] : memref<32x128xf16, 3>
        }
      }
      // Matrix multiplication compute nest.
      affine.for %ii = 0 to 128 step 64 {
        affine.for %kk = 0 to 32 step 16 {
          affine.for %iii = 0 to 64 {
            affine.for %jjj = 0 to 64 {
              affine.for %kkk = 0 to 16 {
                %0 = affine.load %input_fast_buf[%ii + %iii, %kk + %kkk] : memref<128x32xf16, 3>
                %1 = affine.load %weights_fast_buf[%kk + %kkk, %j + %jjj] : memref<32x128xf16, 3>
                %2 = affine.load %output_fast_buf[%ii + %iii, %j + %jjj] : memref<128x128xf32, 3>
                %3 = arith.extf %0 : f16 to f32
                %4 = arith.extf %1 : f16 to f32
                %5 = arith.mulf %3, %4 : f32
                %6 = arith.addf %5, %2 : f32
                affine.store %6, %output_fast_buf[%ii + %iii, %j + %jjj] : memref<128x128xf32, 3>
              }
            }
          } (polyblocks.tile_space)
        } (polyblocks.tile_space)
      } (polyblocks.tile_space)
    } (compute_nest, polyblocks.tile_space)
  } // Output unpacking nest.
  affine.for %ii = 0 to min affine_map<(d0) -> (128, -d0 + 3528)>(xi) {
    affine.for %jj = 0 to 128 {
      %0 = affine.load %output_fast_buf[%ii, %jj] : memref<128x128xf32, 3>
      affine.store %0, %output_memref[(xi + %ii) floordiv 441, ((xi + %ii) mod 441) floordiv 21,
        (xi + %ii) mod 21, %j + %jj] : memref<8x21x21x512xf32>
    } (polyblocks.parallel)
  } (copy_nest, polyblocks.parallel)
} (polyblocks.parallel, polyblocks.tile_space)
} (polyblocks.kind = "matmul")

```

(a) Convolution lowered as 3-d loop matrix multiplication nest using affine accesses.

(b) On-the-fly packing for convolution.

Fig. 7. On-the-fly tiled mapping for convolutions.

4.6 Mapping to matrix units

Several AI chips include specialized hardware to perform matrix-matrix multiplication. PolyBlocks includes a pass that performs the necessary analysis and transformation of affine nests to map from load, store, and compute on elemental-typed memrefs to those of 2-d vector types, which can then be converted to target-specific types. In the case of GPUs, the operations are converted to those on memrefs of subgroup MMA type of size 16x16. We introduced a memref view-like op `polyblocks.matrix_cast` to obtain a view of the memref on 2-d vector types; this view-like op is deabstracted and lowered subsequently soon. As a result of implementing matricization on affine loop nests, we avoid the need to provide a mechanism to implement such a mapping on various kinds of nests like `matmul`, convolutions, `matmuls` within a fused attention nest (as related to Section 4.4), and tensor contractions ensuing from `einsum` computation lowering. A nest mapped to GPU tensor cores is shown in Figure 8.

```

// Grid of thread blocks.
affine.parallel(%arg3) = (0) to (379) {
  %kalloc = memref.alloc() : memref<128x136xf16, 3>
  %kalloc_5 = memref.alloc() (alignment = 16 : i64) : memref<128x16xf16, 3>
  %x7 = memref.vector_cast %kalloc_5 : memref<128x16xf16, 3> to memref<128x2xvector<8xf16>, 3>
  %kalloc_6 = memref.alloc() : memref<128x12xf32, 3>
  affine.parallel(%arg4, %arg5) = (0, 0) to (min(128, %arg3) + -128 + 48400), 3) {
    affine.store %cst_0, %kalloc_6[%arg4, %arg5] : memref<128x12xf32, 3>
  }
  // Warp-level parallelism.
  affine.parallel(%arg4) = (0) to (4) {
    %x8 = affine.apply affine_map<(d0) -> (d0 * 32)>(%arg4)
    %9 = gpu.subgroup_mma_load_matrix %kalloc_5[%x8, %c0] {leadDimension = 12 : index} : memref<128x12xf32, 3> -> !gpu.mma_matrix<32x8xf32, "COp">
    // Threads of a thread block. Copy-in from global memory.
    affine.parallel(%arg5, %arg6) = (0, 0) to (128, 128) {
      %x11 = affine.load %memref_0, ((%arg5 + %arg3 * 128) floordiv 220 + (%arg6 floordiv 3) floordiv 5) mod 224,
        ((%arg5 + %arg3 * 128) mod 220 + %arg6 floordiv 3 - ((%arg6 floordiv 3) floordiv 5) * 5) mod 224, %arg6 mod 3] : memref<1x224x224x3xf16>
      affine.store %x11, %kalloc[%arg5, %arg6] : memref<128x136xf16, 3>
    }
    // Threads of a thread block. Copy-in from global memory.
    affine.parallel(%arg5, %arg6) = (0, 0) to (128, 8) {
      %x11 = affine.load %memref_1[(((%arg5 floordiv 3) floordiv 5) mod 5, (%arg5 floordiv 3) mod 5, %arg5 mod 3, %arg6 mod 3)] : memref<5x5x3xf16>
      affine.store %x11, %kalloc_5[%arg5, %arg6] : memref<128x16xf16, 3>
    }
  }
  // Zero init.
  affine.parallel(%arg5) = (0) to (53) {
    affine.store %cst_47[%arg5 + 75, 0] : memref<128x2xvector<8xf16>, 3>
  }
  %x10 = affine.for %arg5 = 0 to 8 iter_args(%arg6 = %9) -> (!gpu.mma_matrix<32x8xf32, "COp">) {
    %x12 = affine.apply affine_map<(d0) -> (d0 * 16)>(%arg5)
    %x13 = gpu.subgroup_mma_load_matrix %kalloc_5[%x12, %x11] {leadDimension = 136 : index} : memref<128x136xf16, 3> -> !gpu.mma_matrix<32x16xf16, "AOp">
    %x14 = gpu.subgroup_mma_load_matrix %kalloc_5[%x11, %c0] {leadDimension = 16 : index} : memref<128x16xf16, 3> -> !gpu.mma_matrix<16x8xf16, "BOp">
    // Warp-level primitives.
    %x15 = gpu.subgroup_mma_compute %x13, %x14, %arg6 : !gpu.mma_matrix<32x16xf16, "AOp">, !gpu.mma_matrix<16x8xf16, "BOp"> -> !gpu.mma_matrix<32x8xf32, "COp">
    affine.yield %x15 : !gpu.mma_matrix<32x8xf32, "COp">
  }
  gpu.subgroup_mma_store_matrix %x10, %kalloc_6[%x8, %c0] {leadDimension = 12 : index} : !gpu.mma_matrix<32x8xf32, "COp">, memref<128x12xf32, 3>
}
memref.dealloc %kalloc_5 : memref<128x16xf16, 3>
memref.dealloc %kalloc : memref<128x136xf16, 3>
// Threads of a thread block. Copy-out to global memory.
affine.parallel(%arg5, %arg6) = (0, 0) to (min(128, %arg3) + -128 + 48400), 3) {
  %x8 = affine.load %kalloc_6[%arg4, %arg5] : memref<128x12xf32, 3>
  %x9 = arith.truncf %x8 : f32 to f16
  affine.store %x9, %memref_3_0, ((%arg4 + %arg3 * 128) floordiv 220, (%arg4 + %arg3 * 128) mod 220, %arg5) : memref<1x220x220x3xf16>
}
memref.dealloc %kalloc_6 : memref<128x12xf32, 3>
}

```

Fig. 8. IR showing an optimized nest mapped to GPU tensor cores with multi-level parallelism encoded.

4.7 Other optimizations

Appendices A.1 and A.2, part of the supplemental material, describe two more optimizations: (1) quantization support and how all optimizations described apply out of the box to it, and (2) overlap of compute with data copy. Other standard transformations like register tiling, generation of data movement code, vectorization, and unrolling are part of our pipeline, and we do not describe these in more detail. All of these passes rely on analysis utilities that determine the amount of temporal and spatial reuse, access pattern analysis (Section 4.1), parallelism estimation, and polyblocks kind information (Appendix A.4). We perform all of these transformations on affine loop nests in S3.

5 Experimental Evaluation

The evaluation was carried out on an NVIDIA A100 GPU and, in some cases, on an NVIDIA A10 GPU (for batch size 1). As the baselines of Torch Inductor or JAX-XLA rely on hand-tuned highly-optimized vendor libraries, our expectation is not to be always better than these baselines, but to be competitive. The libraries from vendors always get a head start in terms of reaching peak performance of hardware and are often optimized for the sizes found in popular models. Thus, getting close to the performance of library-based approaches still demonstrates the power of fully code-generating compilers, and that they are promising for future hardware not well-served by the manually-developed kernel ecosystem. Apart from the presented evaluation, PolyBlocks delivers the same capabilities and optimizations for TensorFlow, and for CPUs and AMD GPUs. All PolyBlocks compiled code evaluated here is fully automatically generated with no manual intervention or auto-tuning, and with same unmodified PyTorch and JAX as input as with eager executors or Inductor/XLA. Compilation times and PyTorch model coverage with PolyBlocks is provided in Appendix A.5.

5.1 Experimental setup

For all benchmarking, we discard a certain number of warmup runs and take the average of the subsequent 10 or 100 runs, depending on execution time lengths. All execution times reported are the sum total NVIDIA Nsight Systems (nsys) kernel execution times. We lock the clocks for the A10 and A100 GPUs to the recommended 1695 MHz and 1410 MHz, respectively, uniformly for all implementations. The CUDA driver version used was 570.86.15 (CUDA 12.8).

All models are inference workloads that are run in the mixed precision mode, i.e., f16 input and fp32 output for all tensor core targeted computation. Torch-eager and Inductor were used with automatic mixed precision (AMP).

5.2 Performance comparison with Torch Inductor and Eager

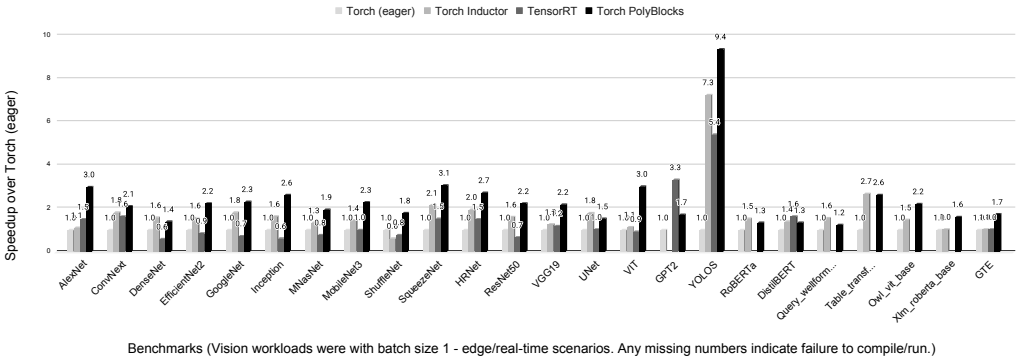


Fig. 9. PyTorch performance with various backends: eager, Inductor, TensorRT, and PolyBlocks. Batch size 1 on the NVIDIA A10. Torch 2.5.1, torch-tensorrt-2.5.0, TensorRT 10.3.0.

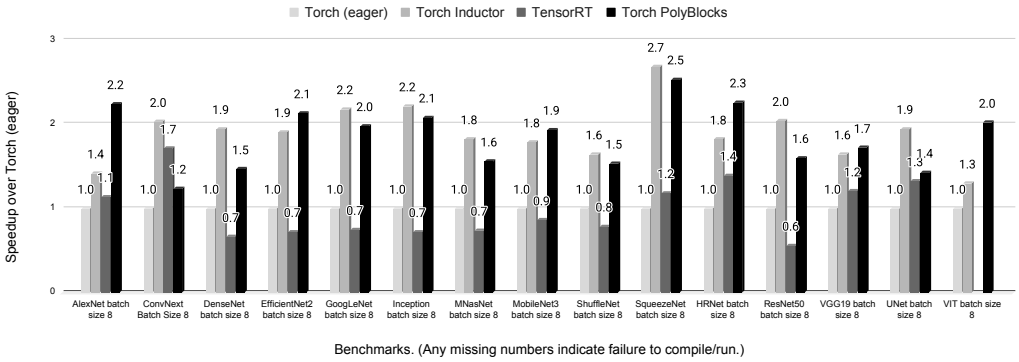


Fig. 10. PyTorch performance with various backends: eager, Inductor, TensorRT, and PolyBlocks. Batch size 8 on the NVIDIA A100. Torch 2.5.1, torch-tensorrt-2.5.0, TensorRT 10.3.0.

We present our evaluation on PyTorch models from Torchvision [32] and Huggingface [12], selected to represent sufficient diversity as far as being based on convolutional networks and transformers, vision and NLP. Figures 9 and 10 show the results on PyTorch models for batch sizes 1 and 8, respectively. While batch size 1 results, reflective of real-time inference, are on the A10 GPU, we use the A100 for batch size 8 which would lead to large utilization and thus more appropriate for a larger GPU.

For batch size one, PyTorch with PolyBlocks as backend on these models is 2.15x as fast on average (geomean) than eager execution, and 1.4x as fast as Inductor and 2.4x as fast as TensorRT. The benefits come from more or better fusion as well as better code generated in some cases for individual operators as will be shown in Section 5.4.

For batch size 8, PolyBlocks is once again 1.8x as fast as eager on average (geomean), and on par (0.97x) with Inductor. In general, we observe that improvements over Inductor are higher with lower batch sizes. This is primarily because the underlying libraries used by Torch Inductor are optimized for larger batch sizes.

5.3 JAX with PolyBlocks

For JAX we use Scenic models [16] and we use JAX-mixed-precision (JMP) [15] to specify a similar mixed precision mode. The mode is specified by setting a JMP policy as `policy = jmp.get_policy("float16")` and subsequently casting the model weights to f16 using `policy.cast_to_params(model_weights)`. We observed that this along with the f16 inputs was sufficient to trigger mixed-precision kernels for JAX-XLA and JAX eager execution.

The PolyBlocks compiler engine with the same pass pipelines is able to compile JAX with a single-line annotation like XLA does. We include a limited set of models with JAX. Table 1 shows that JAX with PolyBlocks is 2.12x (geomean) as fast as JAX eager execution and 1.15x as fast as XLA, an established compiler backend for JAX.

Table 1. JAX with XLA vs PolyBlocks. On NVIDIA A100, JAX 5.0 (Jan 2025) with CUDA 12.9, Flax 0.10.4.

Workload	JAX execution time (ms)			Speedup with PolyBlocks	
	eager	XLA	PolyBlocks	over eager	over XLA
Resnet Batch 8	6.3	2.97	1.87	3.37	1.59
Unet Batch 8	84.6	60.1	69.1	1.22	0.87
Vit Batch 8	10.6	5.09	4.59	2.32	1.11

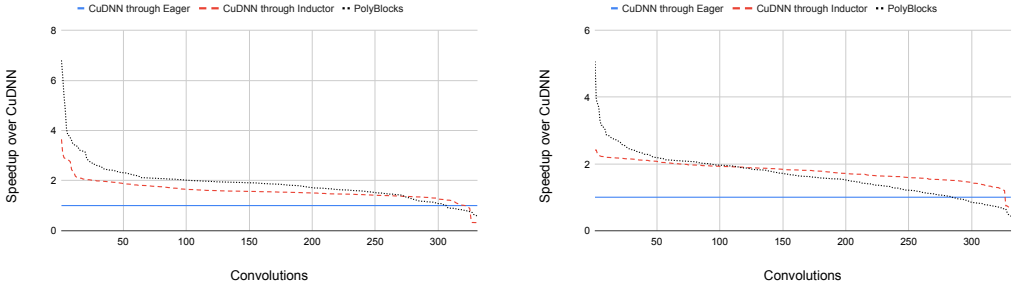
5.4 Individual operator performance: convolutions and matmuls

While cross-operator fusion is the key strength of a compiler, compiler-generated code will not perform well if its generated code is not optimized for individual operators, especially for the compute-intensive ones that provide significant opportunity to improve arithmetic intensity. We typically expect compiler-generated code to be within 1.5x to 2x of the fastest libraries on individual operators so that the benefits from fusion are noticeable.

Figure 11 compares the performance of PolyBlocks with that of CuDNN on hundreds of convolutions drawn from a large number of vision models, including those evaluated above. For convolutions, both torch-eager and inductor use cuDNN. Inductor uses triton for pointwise kernels fusing any surrounding ones, while eager uses cuDNN. The results show that the performance obtained by code generation through the composition of transformations in PolyBlocks is competitive with that of CuDNN in a large number of cases. For several cases (nearly 50), it beats the library by more than 2x.

Similarly, we compare performance on a single matmul operator for various sizes in Figure 12. Here, we compare with Triton and CuBLAS, representative of state-of-the-art mid- and low-level approaches known to reach close to machine peak performance. We obtain performance very close to CuBLAS' on average.

Performance on the attention layer. Table 2 shows the impact of optimizations described in Section 4.4 on various attention layer configurations drawn from transformer-based models. Nsight Systems profile confirms that Torch Inductor uses hand-written flash attention kernels onto which



(a) A10, batch size 1.

(b) A100, batch size 8.

Fig. 11. Performance of convolution operator code generated fully with PolyBlocks on convolutions sourced from various AI models. cuDNN 9.10.2, PyTorch 2.9.0+cu128.

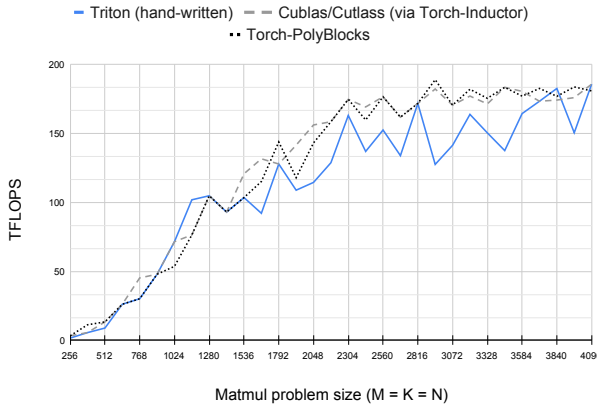


Fig. 12. Performance comparison: CuBLAS, Triton, and PyTorch-PolyBlocks on a single matmul on NVIDIA A100. PyTorch 2.7.1. OpenAI Triton 3.3.1. CuBLAS 12.6.4.1.

it maps the attention layer. The results show the automatic optimization cover significant ground making the generated code’s performance competitive with the state-of-the-art.

5.5 Impact of key optimizations: ablation study

We now isolate the individual impact of certain optimizations and related hardware features. Table 3 data shows how well-optimized code behaves with and without tensor core capability, cross-operator fusion, and reduce-reduce fusion. Tensor cores deliver a geomean speedup of 17x. A100 has a peak 312 mixed precision TFLOPS using tensor cores versus 19.5 TFLOPS using fp32. Also, fp16 data types with fusion lead to 2x as fast movement of tensors to and from global memory. Higher than 16-20x speedups in some cases can be considered anomalies due to CUDA core-targeted code not being optimized as well by the remaining passes of our pipeline. Separately, cross-operator fusion delivers a 2.87x improvement for otherwise fully optimized code, showing the importance of reducing global memory roundtrips and hiding inherently memory-bandwidth bound operations by exploiting on-chip shared memory or register reuse. The table also shows the impact reduce-reduce and wmma fusion have for workloads with the attention layer, isolating the impact of Section 4.4 on full workloads.

Table 2. Attention layer performance for configurations drawn from various models. RR-fusion is reduce-reduce fusion. Torch 2.9.0, CUDA 12.8. NVIDIA A100. Execution times are in milliseconds.

Problem size (batch, num-heads, sequence length, dimensionality of head)	PolyBlocks			Inductor	PolyBlocks speedup over Inductor		
	No fusion	Only rr-fusion	rr+wmma fusion		No fusion	Only rr-fusion	rr+wmma fusion
B=1, H=16, N=512, D=64	0.0671	0.0516	0.0253	0.0174	0.26	0.34	0.69
B=1, H=16, N=2048, D=64	1.7821	0.4770	0.2002	0.1266	0.07	0.27	0.63
B=1, H=16, N=8192, D=64	487.12	6.2722	2.4359	1.5591	0.00	0.25	0.64
B=1, H=16, N=512, D=128	0.0854	0.1124	0.0417	0.0449	0.53	0.40	1.08
B=1, H=16, N=2048, D=128	1.8915	1.0164	0.3024	0.2296	0.12	0.23	0.76
B=1, H=16, N=8192, D=128	487.82	13.016	3.6674	2.7657	0.01	0.21	0.75
DPT-large B=1, H=16, N=577, D=64	0.2059	0.1013	0.0446	0.0236	0.11	0.23	0.53
GPT2 B=1, H=12, N=10, D=64	0.0168	0.0078	0.0078	0.0082	0.49	1.06	1.06
YOLOs B=1, H=6, N=297, D=64	0.0329	0.0248	0.0185	0.0149	0.45	0.60	0.81
RoBERTa B=1, H=16, N=14, D=64	0.0151	0.0081	0.0081	0.0083	0.55	1.03	1.03
DistilBERT B=1, H=12, N=13, D=64	0.0180	0.0081	0.0081	0.0083	0.46	1.02	1.02
QueryWellFormed B=1, H=80, N=14, D=64	0.0157	0.0084	0.0084	0.0085	0.54	1.01	1.01
tabletransf. B=1, H=8, N=500, D=32	0.0424	0.0402	0.0165	0.0155	0.37	0.38	0.84
table_transf. B=1, H=8, N=15, D=32	0.0144	0.0073	0.0073	0.0085	0.45	0.89	0.89
owl-vit B=1, H=16, N=577, D=64	0.2059	0.1013	0.0446	0.0236	0.11	0.23	0.53
owl-vit B=1, H=16, N=16, D=64	0.0142	0.0077	0.0074	0.0083	0.58	1.07	1.13
xlm-roberta B=1, H=12, N=15, D=64	0.0154	0.0081	0.0081	0.0082	0.54	1.02	1.02
gte-attn B=1, H=48, N=10, D=64	0.0173	0.0081	0.0081	0.0084	0.49	1.04	1.04
mpT7b B=1, H=32, N=1024, D=128	0.9601	0.5247	0.1709	0.1235	0.13	0.24	0.72

6 Related Work

The work on BLIS [31, 56] showed how peak hardware performance could be achieved for matrix-matrix multiplication on CPUs in a more modular and reusable way, with cost models and additional tooling. Early evidence of achieving close to peak performance on par with the best hand-written libraries completely using MLIR code generation for CPUs and GPUs, albeit in a preliminary setting, was soon demonstrated [7, 27].

There have been a large number of deep learning compiler efforts in the past decade. Many of these were comprehensively evaluated by Ansel et al. [2]. Torch Inductor was shown to be vastly better both in compilation coverage and in performance on GPUs and CPUs [2]. Prior work compared there included nvFuser [50], NNC [66], XLA [48], ONNXRT [39], TVM [10], and Hidet [17]. A good part of our evaluation was thus focused on using Inductor as a reference for the state-of-the-art for PyTorch.

High-level AI compilers: XLA [24] and Torch Inductor [2] are the prominent production-strength high-level compilers available as part of the respective official repositories. While XLA serves JAX and TensorFlow, Inductor is for PyTorch and potentially other frameworks that can be rewritten to torch graphs. They provide high compilation coverage and the desired level of automation. Models that work with eager execution typically work out of the box and unmodified with JIT compilation turned on. Both XLA and Inductor differ vastly from PolyBlocks in the intermediate representation used to perform transformations. While Inductor uses its own IR abstractions (torch fx IR with aten operations) before relying on Triton for GPU compilation, XLA uses the HLO [63] representation for its high-level transformations before using Triton and LLVM emitters for CPUs/GPUs or LLO for TPUs [20]. Both of these compilers heavily rely on vendor libraries or other open-source kernels for compute-intensive operators on GPUs: CuDNN for convolutions, CuBLAS for matmuls, and various flash attention kernels for the attention layer.

Table 3. Torch-PolyBlocks performance impact of key optimizations isolated. On the A100.

Model	Execution times (milliseconds)					Speedup (with all opts) over			
	w/o tensor-core	w/o fusion	w/o rr fusion	w/o wmma fusion	All opts	no-tensor-core	no-fusion	no-rr-fusion	no-wmma-fusion
AlexNet	2.11	0.35	0.28	0.28	0.28	7.57	1.24	1.00	1.00
ConvNext	12.32	2.83	0.94	0.93	0.93	13.20	3.03	1.01	1.00
DenseNet	9.14	5.31	2.26	2.27	2.23	4.11	2.39	1.02	1.02
EfficientNet2	11.82	4.87	1.42	1.42	1.40	8.43	3.47	1.01	1.01
GoogLeNet	4.19	2.02	0.57	0.57	0.55	7.65	3.68	1.03	1.04
Inception	9.11	3.38	1.01	1.01	0.99	9.20	3.41	1.02	1.02
MNASNet	2.00	1.96	0.43	0.43	0.42	4.81	4.72	1.04	1.04
MobileNet3	1.65	2.10	0.46	0.46	0.45	3.67	4.68	1.03	1.03
ShuffleNet	2.34	2.14	0.54	0.55	0.53	4.44	4.06	1.02	1.03
SqueezeNet	1.40	0.49	0.18	0.18	0.18	7.74	2.73	1.01	1.01
HRNet	21.06	12.19	4.41	4.40	4.07	5.17	2.99	1.08	1.08
ResNet50	7.24	2.03	0.59	0.59	0.59	12.34	3.46	1.01	1.01
VGG19	19.63	1.36	1.00	1.00	0.98	20.12	1.40	1.02	1.02
UNet	192.8	5.12	2.15	2.15	2.10	91.83	2.44	1.02	1.02
VIT	59.96	5.24	2.38	2.21	2.19	27.33	2.39	1.09	1.01
GPT2	114.43	15.29	6.43	7.96	7.93	14.43	1.93	0.81	1.00
YOLOS	86.03	3.99	1.36	1.32	1.22	70.77	3.28	1.12	1.08
RoBERTa	202.9	12.61	5.89	5.88	6.41	31.66	1.97	0.92	0.92
DistilBERT	23.28	2.25	0.95	1.15	1.13	20.64	1.99	0.85	1.02
Query wellformedness score	46.52	4.51	1.83	1.86	1.94	23.93	2.32	0.94	0.96
Stable diffusion turbo unet	462.0	43.72	29.01	17.14	14.6	31.74	3.00	1.99	1.18
Stable diffusion XL1 base unet	7181	720.3	1701	156.8	137.9	52.09	5.23	12.34	1.14
Stable diffusion XL1 refiner unet	7422	1052.6	3889	176.0	155.0	47.88	6.79	25.09	1.14
Flux transformer	33438	2168.9	13510	696.7	451.3	74.09	4.81	29.93	1.54
Table Transformer	66.08	5.37	2.21	2.27	2.37	27.83	2.26	0.93	0.95
OWL VIT Base Patch	138.76	10.35	4.88	3.92	3.16	43.93	3.28	1.55	1.24
DPT Large	496.14	0.00	47.72	43.59	42.12	11.78	0.00	1.13	1.03
XLNet Roberta	187.39	7.72	3.30	3.44	3.44	54.46	2.24	0.96	1.00
GTE	14.72	3.65	1.30	1.75	0.94	15.63	3.87	1.38	1.86
MPT-7B	516.74	22.87	18.95	18.44	18.45	28.00	1.24	1.03	1.00
Geomean speedup						17.36	2.87	1.42	1.07

In contrast, PolyBlocks is fully code generating and the benefits of this approach were discussed in more detail in Section 2. While the work on PyTorch-2 [2] was a milestone result in compilation and auto-parallelization, the resulting infrastructure is not easily reusable for other programming frameworks and hardware due to its choice of multiple IRs and reliance on libraries to perform some of the heavy lifting. The optimizations we described in Sections 4.2, 4.5, and 4.4 are not only not performed in Inductor and XLA, but are difficult to achieve due to the nature and level of IR abstractions available. While our fusion approach is similar in spirit to that of Halide [36, 49] in allowing redundant computation and the choice of depth to compute at, it differs in its choice of intermediate representation, the machinery used to automatically compute slices, cost models, and applicability to n-dimensional affine nests (perfect or imperfect) as opposed to only image processing computations targeted by Halide.

Mid-level compilers: In recent years, mid-level programming frameworks such as Triton [40, 55] have become popular and inspired other similar frameworks [25, 46, 51]. Such frameworks make programmers use tile-level abstractions. Since programmers still perform the tiling and fusion

themselves, considerable effort is needed to express medium to large graphs of computations. On the other hand, high-level frameworks like Inductor, XLA, or PolyBlocks would perform tiling and fusion transparently and automatically. The optimizations we described in Sections 4.2, 4.5, 4.4, as well as quantization (Appendix A.1) are not performed in Triton, and are expected to be performed by the programmer with considerable effort. Mid-level frameworks are thus more suitable as kernel-writing languages to substitute out compute-intensive parts of a graph that were otherwise a bottleneck with high-level approaches. We expect these approaches to co-exist with both lower- and high-level approaches. While FlexAttention [18] is able to generate various configurations of attention, it is restricted to that class of computations. Our approach is more general, but does not yet support the entire cross product of attention configurations with a few aspects left for future implementation in the relevant passes that perform the reduce-reduce fusion described in Section 4.4.

IREE [54] is an MLIR-based deep learning compiler effort with similar goals on certain aspects, such as code generation, as PolyBlocks. However, it differs significantly from PolyBlocks in its choice of dialects and types to perform mid-level optimizations. Based on the evaluation provided in Appendix A.3, it does not provide the level of transformation capability or model coverage as Inductor, XLA, or PolyBlocks for GPUs, with certain basic optimization techniques missing.

Polyhedral works: Several works in the polyhedral compilation literature developed frameworks to perform optimizations for parallelism and locality in both general-purpose and domain-specific settings [6, 9, 19, 22, 37, 57, 60, 64, 65]. These works use the mathematical notion of domains and schedules, as integer sets and affine functions (or relations) respectively, to represent, compose, and apply transformations. IR materializes only after the polyhedral AST generation step. The approach of PolyBlocks is drastically different from being built like a standard compiler pass pipeline where optimizations are performed using both affine analysis and SSA in smaller steps. This allows for more modular and scalable compiler development and testing, better interaction with SSA concepts, and significantly faster compile times. Separately, the fusion approach we have used is fundamentally different from polyhedral loop fusion approaches, which are not slicing based. To our knowledge, the work of Zhao et al. [64] is among the most sophisticated works on tiling and fusion using the polyhedral approach. This approach improves upon or subsumes various prior approaches by combining tiling and fusion with backward slicing. However, the approach uses full-fledged integer set computations and is expensive in comparison to ours. It was also evaluated on smaller benchmarks compared to the ones we used here (cf. Section 5.5). Scalability would thus be a challenge to inputs with hundreds to thousands of nests. In contrast, our approach relies on both SSA and MLIR’s dependence constraints in its flat value constraints form to construct slices easily for the domain of affine nests we encountered.

7 Conclusions

We presented the design and implementation of PolyBlocks, a modular and reusable MLIR-based compiler infrastructure for AI programming frameworks and accelerator chips. PolyBlocks uses sequences of pass pipelines that perform transformations on loop nests, static single assignment (SSA), and multidimensional memory accesses primarily using lightweight affine analysis. Simple transformations are composed together in specialized ways to realize advanced transformations by the use of analytical cost models and heuristics. The developed passes perform transformations related to multi-level tiling, fusion, on-chip scratchpad usage, mapping matmuls and convolutions to matrix units, fusing attention layer computation, and several other well-known transformations for parallelism and locality specialized for dense tensor computations. Experimental results from evaluating PolyBlocks-based compiler backends for PyTorch and JAX for NVIDIA GPUs show that it is able to match or outperform Torch Inductor and XLA by significant margins in several

cases, despite the latter relying on a combination of libraries and code generation. For individual compute-intensive operators, PolyBlocks-based compiler code is competitive with vendor-tuned libraries or kernels written in mid-level frameworks such as Triton. The design and architecture of PolyBlocks provide a way to quickly build new compilers for computations expressed in frameworks like PyTorch and JAX targeting new chips with specialized features.

Acknowledgments

We would like to acknowledge community contributions to various open-source projects that PolyBlocks uses, including MLIR, torch-mlir, and LLVM. We would also like to acknowledge the contributions of Prathamesh Tagore and Vinayaka Bandishti at the time they were employed at Polymage Labs.

References

- [1] Martín Abadi, Ashish Agarwal, Paul Barham, Eugene Brevdo, Zhifeng Chen, Craig Citro, Greg S. Corrado, Andy Davis, Jeffrey Dean, Matthieu Devin, Sanjay Ghemawat, Ian Goodfellow, Andrew Harp, Geoffrey Irving, Michael Isard, Yangqing Jia, Rafal Jozefowicz, Lukasz Kaiser, Manjunath Kudlur, Josh Levenberg, Dandelion Mané, Rajat Monga, Sherry Moore, Derek Murray, Chris Olah, Mike Schuster, Jonathon Shlens, Benoit Steiner, Ilya Sutskever, Kunal Talwar, Paul Tucker, Vincent Vanhoucke, Vijay Vasudevan, Fernanda Viégas, Oriol Vinyals, Pete Warden, Martin Wattenberg, Martin Wicke, Yuan Yu, and Xiaoqiang Zheng. 2015. TensorFlow: Large-Scale Machine Learning on Heterogeneous Systems. <https://www.tensorflow.org/> Software available from tensorflow.org.
- [2] Jason Ansel, Edward Yang, Horace He, Natalia Gimelshein, Animesh Jain, Michael Voznesensky, Bin Bao, Peter Bell, David Berard, Evgeni Burovski, Geeta Chauhan, Anjali Chourdia, Will Constable, Alban Desmaison, Zachary DeVito, Elias Ellison, Will Feng, Jiong Gong, Michael Gschwind, Brian Hirsh, Sherlock Huang, Kshiteej Kalambarkar, Laurent Kirsch, Michael Lazos, Mario Lezcano, Yanbo Liang, Jason Liang, Yinghai Lu, C. K. Luk, Bert Maher, Yunjie Pan, Christian Puhresch, Matthias Reso, Mark Saroufim, Marcos Yukio Siraichi, Helen Suk, Shunting Zhang, Michael Suo, Phil Tillet, Xu Zhao, Eikan Wang, Keren Zhou, Richard Zou, Xiaodong Wang, Ajit Mathews, William Wen, Gregory Chanan, Peng Wu, and Soumith Chintala. 2024. PyTorch 2: Faster Machine Learning Through Dynamic Python Bytecode Transformation and Graph Compilation. In *Proceedings of the 29th ACM International Conference on Architectural Support for Programming Languages and Operating Systems, Volume 2*. 929–947.
- [3] NVIDIA Inc. authors. 2019. CUTLASS Convolution: Implicit GEMM Algorithm. https://docs.nvidia.com/cutlass/media/docs/cpp/implicit_gemm_convolution.html#implicit-gemm-algorithm. Accessed: 10 November 2025.
- [4] NVIDIA Inc. authors. 2025. NVIDIA PTX async copy operations. <https://docs.nvidia.com/cuda/parallel-thread-execution/#data-movement-and-conversion-instructions-non-bulk-copy>.
- [5] Cedric Bastoul. 2004. Code Generation in the Polyhedral Model Is Easier Than You Think. In *Proceedings of the 13th International Conference on Parallel Architectures and Compilation Techniques (PACT '04)*. IEEE Computer Society, Washington, DC, USA, 7–16. doi:10.1109/PACT.2004.11
- [6] Somashekaracharya G. Bhaskaracharya, Julien Demouth, and Vinod Grover. 2020. Automatic Kernel Generation for Volta Tensor Cores. *CoRR* abs/2006.12645 (2020). arXiv:2006.12645 <https://arxiv.org/abs/2006.12645>
- [7] Uday Bondhugula. 2020. High Performance Code Generation in MLIR: An Early Case Study with GEMM. *CoRR* abs/2003.00532 (2020). arXiv:2003.00532 <https://arxiv.org/abs/2003.00532>
- [8] Uday Bondhugula, M. Baskaran, Sriram Krishnamoorthy, J. Ramanujam, A. Rountev, and P. Sadayappan. 2008. Automatic Transformations for Communication-Minimized Parallelization and Locality Optimization in the Polyhedral Model. In *CC*. 132–146.
- [9] Uday Bondhugula, Albert Hartono, J. Ramanujam, and P. Sadayappan. 2008. A practical automatic polyhedral parallelizer and locality optimizer. In *Proceedings of the ACM SIGPLAN 2008 Conference on Programming Language Design and Implementation, Tucson, AZ, USA, June 7-13, 2008*. 101–113. doi:10.1145/1375581.1375595
- [10] Tianqi Chen, Thierry Moreau, Ziheng Jiang, Lianmin Zheng, Eddie Yan, Meghan Cowan, Haichen Shen, Leyuan Wang, Yuwei Hu, Luis Ceze, Carlos Guestrin, and Arvind Krishnamurthy. 2018. TVM: an automated end-to-end optimizing compiler for deep learning. In *Proceedings of the 13th USENIX Conference on Operating Systems Design and Implementation (Carlsbad, CA, USA) (OSDI'18)*. USENIX Association, USA, 579–594.
- [11] Sharan Chetlur, Cliff Woolley, Philippe Vandermersch, Jonathan Cohen, John Tran, Bryan Catanzaro, and Evan Shelhamer. 2014. cuDNN: Efficient Primitives for Deep Learning. arXiv:1410.0759 [cs.NE] <https://arxiv.org/abs/1410.0759>
- [12] Hugging Face community. 2025. Hugging Face. <https://huggingface.co/huggingface>.

- [13] Tri Dao, Daniel Y. Fu, Stefano Ermon, Atri Rudra, and Christopher Ré. 2022. FLASHATTENTION: fast and memory-efficient exact attention with IO-awareness. In *Proceedings of the 36th International Conference on Neural Information Processing Systems (New Orleans, LA, USA) (NIPS '22)*. Curran Associates Inc., Red Hook, NY, USA, Article 1189, 16 pages.
- [14] Tri Dao, Daniel Y. Fu, Stefano Ermon, Atri Rudra, and Christopher Ré. 2022. FlashAttention: Fast and Memory-Efficient Exact Attention with IO-Awareness. arXiv:2205.14135 [cs.LG] <https://arxiv.org/abs/2205.14135>
- [15] Google DeepMind. 2023. JAX JMP. <https://github.com/google-deeppmind/jmp>.
- [16] Mostafa Dehghani, Alexey Gritsenko, Anurag Arnab, Matthias Minderer, and Yi Tay. 2022. Scenic: A JAX Library for Computer Vision Research and Beyond. In *Proceedings of the IEEE/CVF Conference on Computer Vision and Pattern Recognition (CVPR)*. 21393–21398.
- [17] Yaoyao Ding, Cody Hao Yu, Bojian Zheng, Yizhi Liu, Yida Wang, and Gennady Pekhimenko. 2023. Hidet: Task-Mapping Programming Paradigm for Deep Learning Tensor Programs. In *Proceedings of the 28th ACM International Conference on Architectural Support for Programming Languages and Operating Systems, Volume 2 (Vancouver, BC, Canada) (ASPLOS 2023)*. Association for Computing Machinery, New York, NY, USA, 370–384. doi:10.1145/3575693.3575702
- [18] Juechu Dong, Boyuan Feng, Driss Guessous, Yanbo Liang, and Horace He. 2024. Flex Attention: A Programming Model for Generating Optimized Attention Kernels. arXiv:2412.05496 [cs.LG] <https://arxiv.org/abs/2412.05496>
- [19] Venmugil Elango, Norm Rubin, Mahesh Ravishankar, Hariharan Sandanagobalane, and Vinod Grover. 2018. Diesel: DSL for Linear Algebra and Neural Net Computations on GPUs. In *Proceedings of the 2nd ACM SIGPLAN International Workshop on Machine Learning and Programming Languages (Philadelphia, PA, USA) (MAPL 2018)*. ACM, New York, NY, USA, 42–51. doi:10.1145/3211346.3211354
- [20] Google DeepMind. 2025. How to profile TPU programs. <https://jax-ml.github.io/scaling-book/profiling/>.
- [21] Tobias Grosser, Theodoros Theodoridis, Maximilian Falkenstein, Arjun Pitchanathan, Michael Kruse, Manuel Rigger, Zhendong Su, and Torsten Hoefler. 2020. Fast linear programming through transprecision computing on small and sparse data. *Proc. ACM Program. Lang.* 4, OOPSLA, Article 195 (Nov. 2020), 28 pages. doi:10.1145/3428263
- [22] Tobias Grosser, Sven Verdoolaege, and Albert Cohen. 2015. Polyhedral AST Generation Is More Than Scanning Polyhedra. *ACM Trans. Program. Lang. Syst.* 37, 4, Article 12 (July 2015), 50 pages. doi:10.1145/2743016
- [23] Google Inc. 2019. JAX: Transformable numerical computing at scale. <https://github.com/jax-ml/jax>.
- [24] Google Inc. 2021. XLA (Accelerated Linear Algebra): An open-source compiler for machine learning. <https://openxla.org/xla>.
- [25] Google Inc. 2025. Pallas: a JAX kernel language. <https://docs.jax.dev/en/latest/pallas/index.html>.
- [26] NVIDIA Inc. 2021. NVIDIA TensorRT. <https://developer.nvidia.com/tensorrt>.
- [27] Navdeep Katel, Vivek Khandelwal, and Uday Bondhugula. 2022. MLIR-based code generation for GPU tensor cores. In *Proceedings of the 31st ACM SIGPLAN International Conference on Compiler Construction (Seoul, South Korea) (CC 2022)*. Association for Computing Machinery, New York, NY, USA, 117–128. <https://doi.org/10.1145/3497776.3517770>
- [28] Ken Kennedy and John R. Allen. 2001. *Optimizing compilers for modern architectures: a dependence-based approach*. Morgan Kaufmann Publishers Inc., San Francisco, CA, USA.
- [29] Chris Lattner, Mehdi Amini, Uday Bondhugula, Albert Cohen, Andy Davis, Jacques Pienaar, River Riddle, Tatiana Shpeisman, Nicolas Vasilache, and Oleksandr Zinenko. 2021. MLIR: Scaling Compiler Infrastructure for Domain-Specific Computation. In *International symposium on Code Generation and Optimization (CGO)*. 2–14.
- [30] Stella Laurenzo, Sean Silva, and Yi Zhang. 2021. The Torch-MLIR project. <https://github.com/llvm/torch-mlir>.
- [31] Tze Meng Low, Francisco D. Igual, Tyler M. Smith, and Enrique S. Quintana-Orti. 2016. Analytical Modeling Is Enough for High-Performance BLIS. *ACM Trans. Math. Softw.* 43, 2, Article 12 (Aug. 2016).
- [32] TorchVision maintainers and contributors. 2016. *TorchVision: PyTorch's Computer Vision library*. <https://github.com/pytorch/vision>
- [33] Lei Mao. 2024. CUDA Matrix Multiplication Optimization. <https://leimao.github.io/article/CUDA-Matrix-Multiplication-Optimization/>.
- [34] Maxim Milakov and Natalia Gimelshein. 2018. Online normalizer calculation for softmax. *CoRR* abs/1805.02867 (2018). arXiv:1805.02867 <http://arxiv.org/abs/1805.02867>
- [35] MLIR Community developers. 2021. The MLIR project. <https://mlir.llvm.org>.
- [36] Ravi Teja Mullapudi, Andrew Adams, Dillon Sharlet, Jonathan Ragan-Kelley, and Kayvon Fatahalian. 2016. Automatically Scheduling Halide Image Processing Pipelines. *SIGGRAPH 2016 / ACM Trans. Graph.* 35, 4 (July 2016), 83:1–83:11.
- [37] Ravi Teja Mullapudi, Vinay Vasista, and Uday Bondhugula. 2015. PolyMage: Automatic Optimization for Image Processing Pipelines. In *International Conference on Architectural Support for Programming Languages and Operating Systems (ASPLOS)*. 429–443.
- [38] NVIDIA. 2024. TensorFlow-2.x-Quantization-Toolkit. <https://docs.nvidia.com/deeplearning/tensorrt/archives/tensorrt-861/tensorflow-quantization-toolkit/docs/index.html>.

- [39] ONNXRuntime developers. 2021. ONNX runtime. <https://www.onnxruntime.ai>.
- [40] OpenAI. 2025. Triton: Open-Source GPU programming for neural networks. <https://openai.com/index/triton/>.
- [41] Adam Paszke, Sam Gross, Francisco Massa, Adam Lerer, James Bradbury, Gregory Chillemi, Luca DeVito, Zeming Lin, Alban Desmaison, Luca Antiga, Andreas Kopf, Edward Metzger, Federico Chien, Theing Jiang, Nicolas Lefebvre, Vincent Voillet, Marek Zablocki, Razvan Ionescu, Jonathan Li, Jianying Xu, Edward Chu, Michael Killeen, Jeremy Zukerman, Dmytro Sidorov, Hao Yang, Jun Yuan, Wei Zeng, Zhichao Zhang, Zhongqi Zhang, Tianqi Zhou, and Yang Zhu. 2019. PyTorch: An Imperative Style, High-Performance Deep Learning Library. *Advances in Neural Information Processing Systems* 32 (2019). <https://proceedings.neurips.cc/paper/2019/file/bdbca5868b446a877de2c1fa25d72f10-Paper.pdf>
- [42] Arjun Pitchanathan, Christian Ulmann, Michel Weber, Torsten Hoefler, and Tobias Grosser. 2021. FPL: fast Presburger arithmetic through transprecision. *Proc. ACM Program. Lang.* 5, OOPSLA, Article 162 (Oct. 2021), 26 pages. doi:10.1145/3485539
- [43] LLVM project contributors. 2008. The LLVM project. <https://llvm.org>.
- [44] LLVM project contributors. 2025. ORCv2 Design and Implementation of JIT APIs. <https://llvm.org/docs/ORCv2.html>. Accessed: 10 November 2025.
- [45] MLIR project contributors. 2019. MLIR affine dialect. <https://mlir.llvm.org/docs/Dialects/Affine/>. Accessed: 10 November 2025.
- [46] Meta PyTorch Compiler team. 2025. Helion: A Python-embedded DSL that makes it easy to write fast, scalable ML kernels with minimal boilerplate. <https://github.com/pytorch/helion>.
- [47] PyTorch Team. 2024. PyTorch 2 Export Quantization. https://docs.pytorch.org/ao/stable/tutorials_source/pt2e_quant_ptq.html.
- [48] PyTorch XLA Team. 2023. PyTorch/XLA. <https://github.com/pytorch/xla>.
- [49] Jonathan Ragan-Kelley, Andrew Adams, Dillon Sharlet, Connelly Barnes, Sylvain Paris, Marc Levoy, Saman Amarasinghe, and Frédo Durand. 2017. Halide: Decoupling Algorithms from Schedules for High-performance Image Processing. *Commun. ACM* 61, 1 (Dec. 2017), 106–115. doi:10.1145/3150211
- [50] Christian Sarofoen, Piotr Bialecki, Jie Jiang, Kevin Stephano, Masaki Kozuki, Neal Vaidya, and Stas Bekman. 2022. Introducing nvFuser, a deep learning compiler for PyTorch. <https://pytorch.org/blog/introducing-nvfuser-a-deep-learning-compiler-for-pytorch/>.
- [51] Benjamin F. Spector, Simran Arora, Aaryan Singhal, Daniel Y. Fu, and Christopher Ré. 2024. ThunderKittens: Simple, Fast, and Adorable AI Kernels. arXiv:2410.20399 [cs.LG] <https://arxiv.org/abs/2410.20399>
- [52] PyTorch Team and Contributors. 2024. PyTorch: Tensors and Dynamic Neural Networks in Python. <https://github.com/pytorch/pytorch>. Accessed: 10 November 2025.
- [53] Vijay Thakkar, Pradeep Ramani, Cris Cecka, Aniket Shivam, Honghao Lu, Ethan Yan, Jack Kosaian, Mark Hoemmen, Haicheng Wu, Andrew Kerr, Matt Nicely, Duane Merrill, Dustyn Blasig, Aditya Atluri, Fengqi Qiao, Piotr Majcher, Paul Springer, Markus Hohnerbach, Jin Wang, and Manish Gupta. 2023. CUTLASS. <https://github.com/NVIDIA/cutlass>
- [54] The IREE Authors. 2019. *IREE: Intermediate Representation Execution Environment*. <https://github.com/iree-org/iree>
- [55] Philippe Tillet, H. T. Kung, and David Cox. 2019. Triton: an intermediate language and compiler for tiled neural network computations. In *Proceedings of the 3rd ACM International Workshop on Machine Learning and Programming Languages* (Phoenix, AZ, USA) (MAPL 2019). Association for Computing Machinery, New York, NY, USA, 10–19. doi:10.1145/3315508.3329973
- [56] Field G. Van Zee and Robert A. van de Geijn. 2015. BLIS: A Framework for Rapidly Instantiating BLAS Functionality. *ACM Trans. Math. Softw.* 41, 3, Article 14 (June 2015).
- [57] Nicolas Vasilache, Oleksandr Zinenko, Theodoros Theodoridis, Priya Goyal, Zachary DeVito, William S. Moses, Sven Verdoolaege, Andrew Adams, and Albert Cohen. 2018. Tensor Comprehensions: Framework-Agnostic High-Performance Machine Learning Abstractions. arXiv:1802.04730 [cs.PL] <https://arxiv.org/abs/1802.04730>
- [58] Ashish Vaswani, Noam Shazeer, Niki Parmar, Jakob Uszkoreit, Llion Jones, Aidan N. Gomez, Lukasz Kaiser, and Illia Polosukhin. 2017. Attention is all you need. In *Proceedings of the 31st International Conference on Neural Information Processing Systems* (Long Beach, California, USA) (NIPS’17). Curran Associates Inc., Red Hook, NY, USA, 6000–6010.
- [59] Sven Verdoolaege. 2010. ISL: An Integer Set Library for the Polyhedral Model. In *Proceedings of the Third International Congress Conference on Mathematical Software* (Kobe, Japan) (ICMS’10). Springer-Verlag, Berlin, Heidelberg, 299–302. <http://dl.acm.org/citation.cfm?id=1888390.1888455>
- [60] Sven Verdoolaege, Juan Carlos Juega, Albert Cohen, José Ignacio Gómez, Christian Tenllado, and Francky Catthoor. 2013. Polyhedral Parallel Code Generation for CUDA. *ACM Trans. Archit. Code Optim.* 9, 4, Article 54 (Jan. 2013), 23 pages. doi:10.1145/2400682.2400713
- [61] Sven Verdoolaege and other contributors. 2010. Integer Set Library. <https://libisl.sourceforge.io/>.
- [62] Michael Wolfe. 1995. *High Performance Compilers for Parallel Computing*. Addison-Wesley Longman Publishing Co., Inc., Boston, MA, USA.
- [63] XLA Team. 2025. OpenXLA: XLA operation semantics. https://openxla.org/xla/operation_semantics.

- [64] Jie Zhao, Jinchun Xu, Peng Di, Wang Nie, Jiahui Hu, Yanzhi Yi, Sijia Yang, Zhen Geng, Renwei Zhang, Bojie Li, Zhiliang Gan, and Xuefeng Jin. 2024. Modeling the Interplay between Loop Tiling and Fusion in Optimizing Compilers Using Affine Relations. *ACM Trans. Comput. Syst.* 41, 1–4, Article 5 (Jan. 2024), 45 pages. doi:10.1145/3635305
- [65] Oleksandr Zinenko, Sven Verdoolaege, Chandan Reddy, Jun Shirako, Tobias Grosser, Vivek Sarkar, and Albert Cohen. 2018. Modeling the conflicting demands of parallelism and Temporal/Spatial locality in affine scheduling. In *Proceedings of the 27th International Conference on Compiler Construction (Vienna, Austria) (CC '18)*. Association for Computing Machinery, New York, NY, USA, 3–13. doi:10.1145/3178372.3179507
- [66] Mikhail Zolotukhin. 2021. NNC walkthrough: how PyTorch ops get fused. <https://dev-discuss.pytorch.org/t/nnc-walkthrough-how-pytorch-ops-get-fused/125>.

A Supplemental Material for “PolyBlocks: A Compiler Infrastructure for AI Chips and Programming Frameworks”

A.1 Quantization

PolyBlocks supports PyTorch models quantized using PyTorch 2 export quantization [47] and TensorFlow models quantized using TensorFlow-2.x-Quantization-Toolkit [38]. Optimizations for uniform symmetric int8-quantized models are currently supported. IR extracted from models quantized using both workflows contains quantize and dequantize stub operations without enclosing any compute operations. At the *mhlo* dialect level, in the S1 stage of the pipeline 4, transformation passes reposition compute-intensive operations such as matmuls and convolutions between the quantize and dequantize operations, enabling these operations to be executed in *int8* format. All optimization that works on non-quantized models, like fusion, vectorization, and matrix-unit mapping, works out of the box for quantized models. An example showing the fusion of nearly 15-20 operators into the output of a quantized tensor-core mapped convolution is shown in Figure 16. This example shows tiling, fusion, mapping to tensor cores, and vectorization of on-chip to/from global memory data movement code.

Figures 13 and 14 compare the performance of PolyBlocks with quantization to 8-bit integers. Torch-eager and Inductor have limited support for optimization in the presence of quantization. We thus observe dramatic speedups when using PolyBlocks. Furthermore, Figure 15 demonstrates the benefit with int8 quantization over fp16/fp32, putting the performance with quantization in perspective with other reported performances in Section 5.

PyTorch quantized model performance with Torch (eager), Inductor and PolyBlocks backends
On NVIDIA A10, torch 2.5.1, CUDA 12.8.

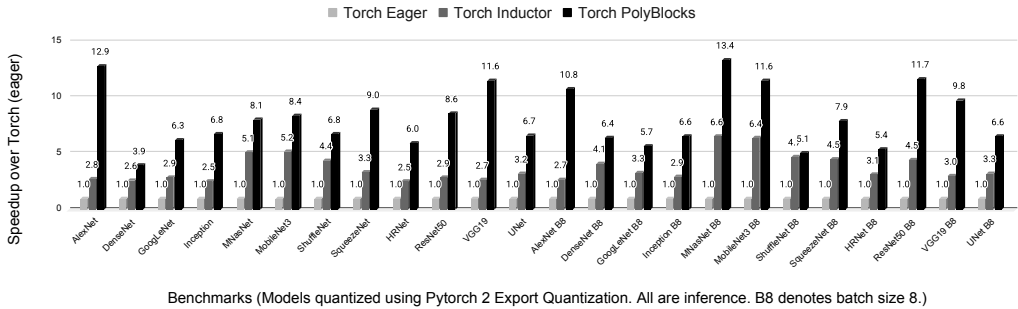


Fig. 13. PyTorch i8 quantized performance with various backends: eager, Inductor, TensorRT, and PolyBlocks. NVIDIA A10. Torch 2.5.1, torch-tensorrt-2.5.0, TensorRT 10.3.0.

A.2 Overlapping compute with data copy

With the increasing disparity between memory bandwidth and compute throughput, it is critical to overlap data movement with compute explicitly for many accelerator chips. Our pass pipeline realizes this through a special pass. The pass is powerful enough to overlap data movement at multiple levels of the memory hierarchy with compute, as is common in modern GPUs. Furthermore, the pass can overlap multiple stages of data movement with compute. The pass leverages an affine-loop-shifting transformation to realize the compute-copy overlap by shifting the data-copy ahead of the compute by the number of stages determined by a heuristic-based analytical cost model. The cost model considers various aspects like tile sizes and the amount of available on-chip memory to determine the number of copy stages to overlap.

PyTorch quantized model performance with Torch (eager), Inductor and PolyBlocks backends

On NVIDIA A100, torch 2.5.1, CUDA 12.8.

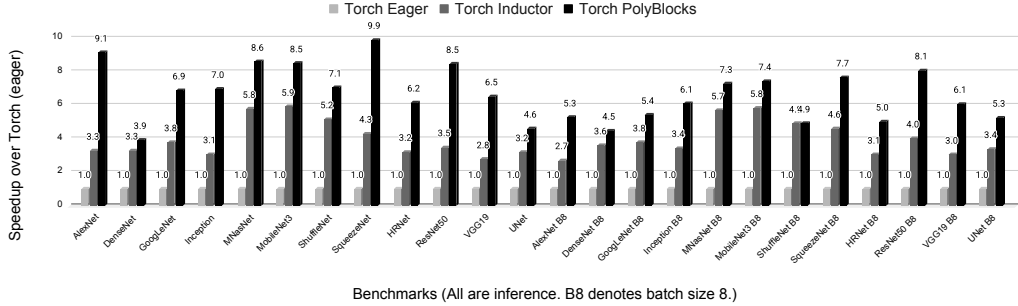


Fig. 14. PyTorch i8 quantized performance with various backends: eager, Inductor, TensorRT, and PolyBlocks. NVIDIA A100. Torch 2.5.1, torch-tensorrt-2.5.0, TensorRT 10.3.0.

PyTorch-PolyBlocks: Improvement with i8 quantization over fp16/32 on an NVIDIA A10

On NVIDIA A10, torch 2.5.1, CUDA 12.8.

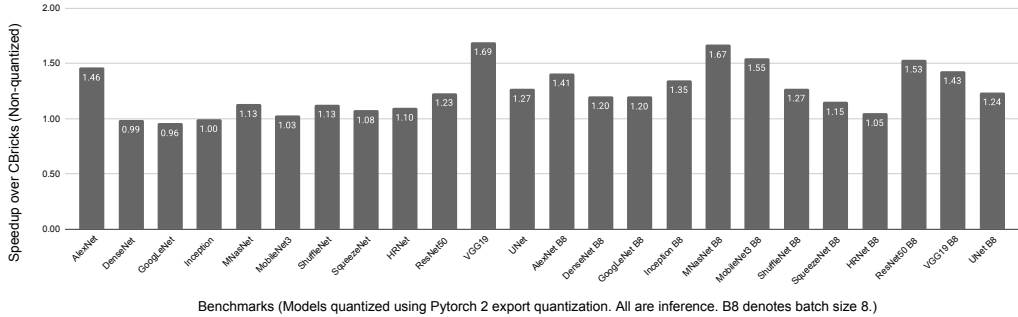


Fig. 15. PyTorch-PolyBlocks i8 quantized performance vs fp16/32: batch size 8 on the NVIDIA A10.

After the shifting transformation, the pass maps the data-movement loops to NVIDIA async-copy operations [4]. As these are asynchronous copy operations (executing thread does not wait for the copy to complete), the pass then inserts necessary synchronization operations to ensure correctness and completes the transformation. Enabling this transformation plays a key role in achieving close to peak performance for unit workloads like matmul, convolutions, and fused-attention.

A.3 Comparison with IREE

We also compare with another MLIR-based code generator, although it has limited coverage and optimization capability. IREE performance in Table 4 shows that its optimizer is missing significant transformations including mapping to tensor cores for non-trivial models. IREE’s frontend integration also failed to lower six of the nine models we were able to try.

A.3.1 IREE setup. Details of the IREE version and setup used for benchmarking are provided below. `iree-base-compiler`, `iree-base-runtime`, `iree-turbine` version 3.8.0 through the official PIP package.

IREE compiler flags:

```

// Tensor core mapped compute on a tile.
...
X520 = gpu.subgroup_mma_compute X508, X519, %arg166 (b_transpose) :
!gpu.mma_matrix<16x16xi8, "A0p">, !gpu.mma_matrix<16x16xi8, "B0p"> ->
!gpu.mma_matrix<16x16xi32, "C0p">
X521 = gpu.subgroup_mma_compute X511, X519, %arg167 (b_transpose) :
!gpu.mma_matrix<16x16xi8, "A0p">, !gpu.mma_matrix<16x16xi8, "B0p"> ->
!gpu.mma_matrix<16x16xi32, "C0p">
affine.yield X510, X512, X514, X515, X517, X518, X520, X521 :
!gpu.mma_matrix<16x16xi32, "C0p">, !gpu.mma_matrix<16x16xi32, "C0p">,
!gpu.mma_matrix<16x16xi32, "C0p">, !gpu.mma_matrix<16x16xi32, "C0p">,
!gpu.mma_matrix<16x16xi32, "C0p">, !gpu.mma_matrix<16x16xi32, "C0p">,
!gpu.mma_matrix<16x16xi32, "C0p">, !gpu.mma_matrix<16x16xi32, "C0p">
}
gpu.barrier
gpu.subgroup_mma_store_matrix X506#0, %view_574[%494, %c0] [leadDimension = 68 : index] : !gpu.mma_matrix<16x16xi32, "C0p">, memref<128x68xi32, 3>
gpu.subgroup_mma_store_matrix X506#1, %view_574[%496, %c0] [leadDimension = 68 : index] : !gpu.mma_matrix<16x16xi32, "C0p">, memref<128x68xi32, 3>
gpu.subgroup_mma_store_matrix X506#2, %view_574[%494, %c16] [leadDimension = 68 : index] : !gpu.mma_matrix<16x16xi32, "C0p">, memref<128x68xi32, 3>
gpu.subgroup_mma_store_matrix X506#3, %view_574[%496, %c16] [leadDimension = 68 : index] : !gpu.mma_matrix<16x16xi32, "C0p">, memref<128x68xi32, 3>
gpu.subgroup_mma_store_matrix X506#4, %view_574[%494, %c32] [leadDimension = 68 : index] : !gpu.mma_matrix<16x16xi32, "C0p">, memref<128x68xi32, 3>
gpu.subgroup_mma_store_matrix X506#5, %view_574[%496, %c32] [leadDimension = 68 : index] : !gpu.mma_matrix<16x16xi32, "C0p">, memref<128x68xi32, 3>
gpu.subgroup_mma_store_matrix X506#6, %view_574[%494, %c48] [leadDimension = 68 : index] : !gpu.mma_matrix<16x16xi32, "C0p">, memref<128x68xi32, 3>
gpu.subgroup_mma_store_matrix X506#7, %view_574[%496, %c48] [leadDimension = 68 : index] : !gpu.mma_matrix<16x16xi32, "C0p">, memref<128x68xi32, 3>
}
affine.parallel (%arg158, %arg159) = (0, 0) to (128, 128) {
%494 = affine.load %493[%arg158, %arg159] : memref<128xi128xvector<4xi32>, 3>
%495 = arith.sitofp %494 : vector<4xi32> to vector<4xf32>
%496 = affine.load %10[%arg159] : memref<16xvector<4xf32>>
%497 = arith.mulf %495, %496 : vector<4xf32>
%498 = affine.load %11[%arg159] : memref<16xvector<4xf32>>
%499 = arith.addf %497, %498 : vector<4xf32>
%500 = arith.divf %499, %cst_35 : vector<4xf32>
%501 = math.roundeven %500 : vector<4xf32>
%502 = arith.maximumf %501, %cst_6 : vector<4xf32>
%503 = arith.minimumf %502, %cst_5 : vector<4xf32>
%504 = arith.fptosi %503 : vector<4xf32> to vector<4xi8>
%505 = arith.sitofp %504 : vector<4xi8> to vector<4xf32>
%506 = affine.load %12[%arg159] : memref<16xvector<4xf32>>
%507 = arith.truncf %cst_61 : f64 to f32
%508 = vector.splat %507 : vector<4xf32>
%509 = arith.addf %506, %508 : vector<4xf32>
%510 = vector.extract %509[0] : vector<4xf32>
%511 = math.sqrt %510 : f32
%512 = vector.insert %511, %509 [0] : f32 into vector<4xf32>
%513 = vector.extract %509[1] : vector<4xf32>
%514 = math.sqrt %513 : f32
%515 = vector.insert %514, %512 [1] : f32 into vector<4xf32>
%516 = vector.extract %509[2] : vector<4xf32>
%517 = math.sqrt %516 : f32 loc(1)loc526
%518 = vector.insert %517, %515 [2] : f32 into vector<4xf32>
%519 = vector.extract %509[3] : vector<4xf32>
%520 = math.sqrt %519 : f32
%521 = vector.insert %520, %518 [3] : f32 into vector<4xf32>
%522 = arith.mulf %505, %cst_35 : vector<4xf32>
%523 = arith.divf %cst_2, %521 : vector<4xf32>
%524 = affine.load %13[%arg159] : memref<16xvector<4xf32>>
%525 = arith.subf %522, %524 : vector<4xf32>
%526 = arith.mulf %525, %523 : vector<4xf32>
%527 = affine.load %14[%arg159] : memref<16xvector<4xf32>>
%528 = arith.mulf %526, %527 : vector<4xf32>
%529 = affine.load %15[%arg159] : memref<16xvector<4xf32>>
%530 = arith.addf %528, %529 : vector<4xf32>
%531 = arith.cmpf ugt, %530, %cst_0 : vector<4xf32>
%532 = arith.select %531, %530, %cst_0 : vector<4xi1>, vector<4xf32>
%533 = arith.divf %532, %cst_34 : vector<4xf32>
%534 = math.roundeven %533 : vector<4xf32>
%535 = arith.maximumf %534, %cst_6 : vector<4xf32>
%536 = arith.minimumf %535, %cst_5 : vector<4xf32>
%537 = arith.fptosi %536 : vector<4xf32> to vector<4xi8>
affine.store %537, %17[%arg157 floordiv 800, ((%arg158 + %arg157 * 128) mod 102400) floordiv 320,
(%arg158 + %arg157 * 128) mod 320, %arg159] : memref<8x320x320xi16xvector<4xi8>
}
}

```

Fig. 16. IR after fusion of de-quantization and quantization at the output of a convolution operator.

```

--iree-codegen-llvmgpu-use-igemm
--iree-codegen-llvmgpu-use-mma-sync
--iree-codegen-llvmgpu-igemm-pad-convolution
--iree-codegen-llvmgpu-use-tile-and-fuse-matmul
--iree-codegen-llvmgpu-use-tile-and-fuse-convolution
--iree-cuda-target-features=+ptx87 --iree-opt-level=03

```

A.4 PolyBlock kinds and attributes

We classify affine nests into four kinds: (1) pointwise, (2) broadcast, (3) matmul (which includes convolutions as well), and (4) miscellaneous affine (‘misc’). These polyblocks kinds are marked as attributes on the root affine nest and then used in some of the passes as hints in guiding to a limited extent some of the optimization choices. PolyBlock kinds are determined primarily from the nature of affine access patterns in relation to the surrounding loop induction variables.

Table 4. Comparison with IREE. IREE version 3.8.0 (PIP). All execution times are in milliseconds.

Workload	IREE (milliseconds)		PolyBlocks (milliseconds)
	fp32 with AMP	fp16	mixed fp16/fp32
Alexnet batch 8	17.92	15.21	0.36
VGG19 batch 8	225.59	189.65	2.81
Unet batch 8	1353.88	1303.28	13.2
DenseNet batch 8	Crash	Crash	3.49
Inception batch 8	Crash	Crash	1.85
Resnet batch 8	Crash	Crash	1.74
Vit batch 8	Fails to lower	Fails to lower	4.51
HRNet batch 8	Fails to lower	Fails to lower	6.37
YOLOs	Fails to lower	Fails to lower	1.21
Geomean speedup with PolyBlocks			65.5x

The absence of these hints is guaranteed not to affect correctness, but only optimizations and performance. As an example, we prevent certain kinds of fusion from happening into matmul nests that may prevent mapping to matrix units when available. Strictly speaking, such analysis can be performed on demand with some additional overhead and code burden. So, the presence of PolyBlocks types can be thought of as for convenience and to reduce additional detection overhead or burden.

We also make use of external attributes to convey optimization information and hints over short distances in the pass pipeline, where distance indicates the number of passes, and avoid recomputation of certain properties. The target information is supplied through module attribute information from the driver (C4 in Section 3.2). The root loops of the nests are marked with the target early in stage S3.

A.5 Compilation times and model coverage

Some of the largest models evaluated in Section 5 involve a few thousand torch aten operators and up to tens of thousands of affine nests in the unoptimized form at the entry point of S3 (Figure 4). Compilation with PolyBlocks is completed in tens of seconds to two minutes, with a few models compiling in a few seconds. For reference, the smallest models such as Alexnet take four seconds to compile through all five stages of PolyBlocks, with 1.7 seconds in the key optimization stage S3. The largest models, such as those of the order of Stable Diffusion XL1 refiner Unet take about 10 minutes to compile, with about 7 minutes spent in stage S3. Most medium-sized models take a few tens of seconds. We thus consider the infrastructure quite scalable from the compilation time standpoint, although there are opportunities to optimize compile times.

Figure 17 shows that PolyBlocks is able to successfully compile and execute 90% of the 205 models that were used in the evaluation in PyTorch-2 work [2], which both torch-eager and Inductor successfully execute. All 10% that fail are due to operator lowering issues in torch-mlir [30] as opposed to core compile engine issues.

PyTorch model coverage with different backends: eager mode vs Inductor (compiled) vs CBricks (compiled)
Torch 2.5.0, CUDA 12.5 on NVIDIA GPUs on an Ubuntu 22.04 LTS x86-64 system.

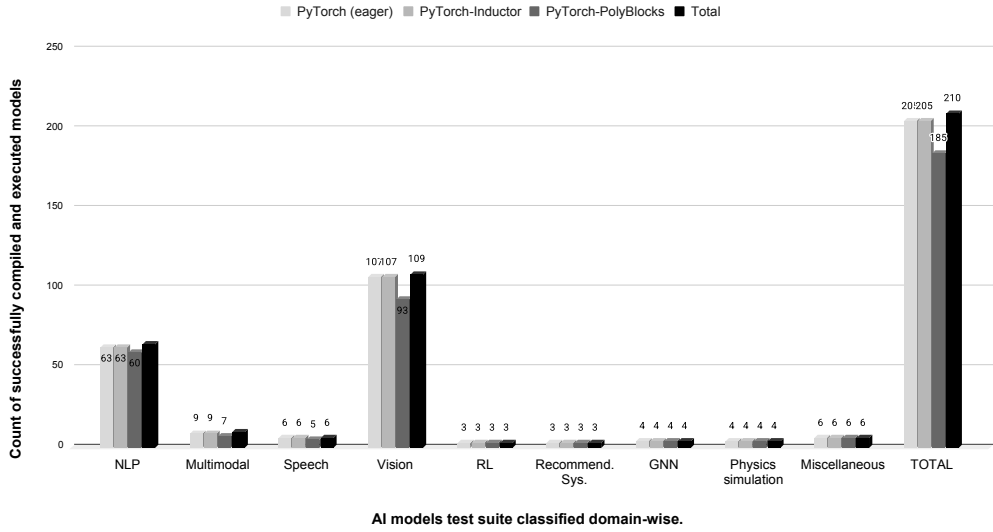


Fig. 17. PyTorch model coverage with PolyBlocks.